Acoustic-Based Door Spacing for the Assessment of *Posidonia oceanica* Biometrics, Habitat Characteristics, and Ecological Status Along the Turkish Mediterranean Coast

Erhan Mutlu *

Posted Date: 12 March 2026

doi: 10.20944/preprints202603.1020.v1

Keywords: vulnerable seagrass; conservative sampling; biometrics and ecological estimates; Levantine Sea

 doi:10.20944/preprints202603.1020.v1

Article

Acoustic-Based Door Spacing for the Assessment of *Posidonia oceanica* Biometrics, Habitat Characteristics, and Ecological Status Along the Turkish Mediterranean Coast

Erhan Mutlu

Akdeniz University, Fisheries Faculty, Main Campus, 07050, Antalya, Turkey; emutlu@akdeniz.edu.tr

Abstract

Seagrasses play a fundamental role as ecosystem engineers and habitat architects in coastal environments. In the Mediterranean Sea, *Posidonia oceanica* is an endemic, vulnerable, and legally protected species that is highly sensitive to environmental degradation and is widely used as an indicator of pristine ecological conditions. Ongoing global warming and increasing anthropogenic pressures highlight the need for precautionary, non-destructive methods to assess *P. oceanica* meadows. Traditional SCUBA-based surveys, although accurate, are time-consuming, labour-intensive, and limited by diver availability and underwater working time, particularly when estimating biometric parameters such as shoot density and leaf length. In this study, we applied a conservative acoustic-based approach to quantitatively estimate *P. oceanica* meadow characteristics, moving beyond purely qualitative acoustic mapping previously restricted to distributional assessments. Acoustic data collected during winter and summer 2015 along the entire Turkish Mediterranean coast were analysed to estimate seagrass biometrics and to derive indicators of ecological status. Acoustic outputs were validated through comparison with SCUBA-diving observations, allowing evaluation of the reliability and cost-effectiveness of the method. The acoustic system enabled rapid, large-scale assessment of seagrass distribution, coverage, habitat structure, and ecological condition, overcoming limitations associated with other remote sensing techniques. The results demonstrate that acoustic data can support the estimation of multiple biometric and ecological parameters and facilitate classification of ecosystem status from poor to high (pristine), in line with updated international assessment criteria. For the first time, this study provides high-resolution spatiotemporal distribution and coverage of *P. oceanica* meadows and associated benthic habitats along a substantial portion of the Turkish Mediterranean coast using acoustics alone. The approach offers a valuable non-destructive alternative for monitoring seagrass ecosystems and supports sustainable conservation and management of Mediterranean coastal habitats.

Keywords: vulnerable seagrass; conservative sampling; biometrics and ecological estimates; Levantine Sea

1. Introduction

Seagrasses play a paramount role in marine ecosystems by providing a wide range of ecological functions. They contribute to biogeochemical cycling, support diverse biological communities by offering habitat and nursery grounds, and enhance coastal stability through sediment trapping and erosion prevention [1]. Owing to these functions, seagrasses are widely recognised as coastal ecosystem engineers and internal architects. In addition, seagrass meadows are effective indicators of ecological status, reflecting interactions between offshore and inshore waters, the presence or absence of anthropogenic pressures, and long-term signals of seawater warming. Among seagrass taxa, *Posidonia* spp. occur in the Mediterranean Sea, the eastern Middle Atlantic, and Australian

 doi:10.20944/preprints202603.1020.v1

coastal waters. However, *Posidonia oceanica* is an endemic species exclusive to the Mediterranean Sea and represents the most widespread and structurally important seagrass in the basin [2-6]. The Mediterranean Sea, the world's largest intercontinental sea, hosts extensive *P. oceanica* meadows along most of its coastlines. Due to its slow growth, longevity, and sensitivity to disturbance, *P. oceanica* is classified as endangered, threatened, and legally protected under several international conventions and frameworks [7-9].

The Mediterranean Sea is characterized by complex circulation patterns and interconnected water masses linked to the Atlantic Ocean, the Red Sea, and the Indo-Pacific through both horizontal and vertical exchanges. These dynamics, together with atmospheric–ocean interactions, climate-driven warming, biological invasions, and ongoing "tropicalization" processes, strongly influence the biometrics, growth, flowering, and spatial distribution of *P. oceanica* [10-12]. As a result, meadow structure and health vary considerably across spatial and temporal scales.

Posidonia oceanica is capable of colonizing a wide range of substrates, from hard bottoms (rock and matte) to soft sediments (sand, gravel, and mud), with substrate type exerting a strong influence on biometric characteristics. The species typically extends from shallow waters to depths exceeding 40 m under favourable environmental conditions. Accordingly, populations are often categorized into shallow (<15 m) and deep (>15 m) assemblages, which exhibit distinct biometric and ecological characteristics [12-14]. Shallow populations, particularly around 15 m depth show higher spatial and temporal variability in biometric parameters, with pronounced seasonal fluctuations often observed during summer months. Sediment enrichment (e.g. elevated total organic carbon) and water-column degradation (e.g. increased nutrient loads leading to reduced light availability) negatively affect growth, shoot density, and meadow persistence. In pristine conditions, shoot density tends to remain within relatively stable ranges at given depth intervals throughout the year [11,15-18]. *P. oceanica* meadows host diverse epiphytic assemblages, including species indicative of both pristine and degraded conditions, and provide feeding grounds for several reptile and fish species. Consequently, accurate knowledge of meadow distribution and structure is essential for ecosystem-based management and conservation, particularly when achieved without damaging sampling practices [10,12-14].

Extensive in situ and ex situ studies on *P. oceanica* ecology, physiology, and distribution have been conducted in the western Mediterranean (e.g. [9, 18-22]. In contrast, studies from the eastern Mediterranean, particularly along the Levantine Basin and the Turkish coast, remain comparatively limited. Although recent investigations have addressed distribution, ecology, and growth parameters in parts of the Turkish Mediterranean [12-14], significant knowledge gaps persist, especially along the easternmost Mediterranean coastline. Greek waters, however, have been more intensively studied than other eastern Mediterranean regions (e.g. [16, 23-28]).

Traditionally, *P. oceanica* studies have relied heavily on SCUBA-based sampling, which can be locally destructive and potentially harmful to meadow integrity [13, 29-30]. To mitigate impacts, strict recommendations on shoot collection limits have been proposed [13, 29-30]. Nevertheless, the need for non-destructive and large-scale monitoring approaches has driven the increased use of remote sensing techniques, including underwater video, aerial and satellite imagery, and acoustic systems. These methods have been widely applied to map seagrass distribution, coverage, and canopy height across the Mediterranean [31-35].

Visual remote sensing techniques, particularly satellite-based approaches, have benefited from the launch of Sentinel-2, enabling broad-scale mapping and calibration through sea-truthing (e.g. [36-39]). However, these techniques are constrained by atmospheric conditions, water clarity, and light penetration, unlike acoustic systems, which rely on sound waves and can operate independently of optical limitations [40-43]. Vegetation acoustics have historically been used primarily for qualitative mapping of seagrass and macroalgal distribution using side-scan sonar and echosounders [32, 34,44-45]. Early acoustic applications were limited by ambiguity in scatterer identification [46-47]. Recent advances, however, have enabled the integration of acoustic scattering properties, multi-frequency responses, and target-specific characteristics to improve species discrimination [48-51]. Quantitative

 doi:10.20944/preprints202603.1020.v1

calibration studies have further strengthened relationships between acoustic signals and seagrass biometric parameters [52-55]. Building on these developments, Mutlu and colleagues characterized the acoustic scattering properties of *P. oceanica* and *Cymodocea nodosa*, developed the "SheathFinder" algorithm [56], and introduced the "POSIBIOM" script package to estimate *P. oceanica* leaf biomass and length from acoustic data [49, 50-51, 57]. Preliminary comparisons between acoustic estimates and SCUBA-derived biometrics were conducted in the Antalya–Manavgat region [58].

Although coarse distribution maps of seagrass meadows exist for Turkish waters, comprehensive quantitative assessments remain lacking. Using leaf biomass estimated acoustically and biomass–biometric relationships derived from SCUBA samples, the present study aims to map *P. oceanica* distribution and estimate key biometric parameters (shoot density, leaf biomass, number of leaves, leaf length, leaf area, and leaf area index), assess seasonal and depth-related variability, and evaluate ecological status along the entire Turkish Mediterranean coast using winter and summer 2019 data. For the first time, this study provides high-resolution, acoustics-only mapping of *P. oceanica* meadows across previously unstudied sections of the Mediterranean coastline, significantly improving regional knowledge beyond traditional SCUBA-based surveys.

2. Material and Methods

Material and Methods include acoustical data collection, quantitative seasonal relationships established between biometrics and the acoustical Elementary Distance Sampling Unit (EDSU) [50] for POSIBIOM analyses [49], generation of biometrics–biomass relationships from SCUBA sampling, followed by acoustical estimation of biometrics and ecology with environmental parameters introduced for the study area [13-14]) in winter (December 2018–January 2019) and summer (June–July 2019). Each survey lasted two months.

2.1. Study Area Environment

The study area environment was previously described by Mutlu et al. [13-14] as follows. Half of the stations in region 3 (Muğla Bay) were influenced by Aegean Sea waters, and almost half of the total stations were located in region 2 (Antalya Bay). Western stations of region 1 and all stations in region 2 (Mersin Bay) were situated within the Atlantic rim current of Levantine waters, which strongly influences environmental parameters (Figure 1).

Bottom-depth distribution of SCUBA sampling sites generally varied between 10 and 30 m, while depths of 5 and 35 m were rarely included. Regional average bottom depths were 17.9 m and 20.8 m in region 3 (Muğla), 19.5 m and 18.9 m in region 1 (Antalya), and 16.0 m and 18.4 m in region 2 (Mersin) in winter and summer, respectively. Bottom types were mainly composed of sand and mud in region 3, rocks in region 1, and matte and mud in region 2.

2.2.1. Water Physics

Average sea surface salinity increased from west to east and varied between 37.2 and 38.9 PSU in winter. In summer, salinity reached its minimum in region 1 (Antalya), its maximum in region 3 (Muğla), and intermediate values in region 2 (Mersin). Sea surface salinity was generally lower in winter than in summer. Near-bottom water salinity was lower in summer (36.0–37.2 PSU) than in winter (38.4–38.8 PSU) and increased from west to east, in contrast to its standard deviation.

Sea surface temperature increased from 16.7 °C in the west to 18.8 °C in the east in winter, and from 24.9 °C (region 3) to 26.9 °C (region 1), followed by 26.0 °C (region 2), in summer. Near-bottom water temperature showed similar regional trends in both seasons and varied between 16.9 °C and 19.6 °C in winter and between 23.5 °C and 25.4 °C in summer. Dissolved oxygen, measured only in winter due to probe malfunction in summer, showed an increasing trend from east (9.3 mg L^{-1}) to west (9.8 mg L^{-1}). Sea surface and near-bottom oxygen values were similar. pH ranged between 8.0 and 9.1 in winter and between 8.5 and 9.5 in summer.

 doi:10.20944/preprints202603.1020.v1

In winter, sea surface waters were denser within the rim current (more saline and temperate) than in semi-enclosed gulfs (Antalya, Yeşilova, and Hisarönü gulfs), which were less saline and temperate. In summer, sea surface water density increased from east to west. Eastern waters were slightly more saline and warmer, reducing density, whereas western waters were less temperate, increasing density relative to eastern sampling sites. This pattern suggests stronger Aegean Sea influence in the west, which was also expected to affect *P. oceanica* biometric characteristics.

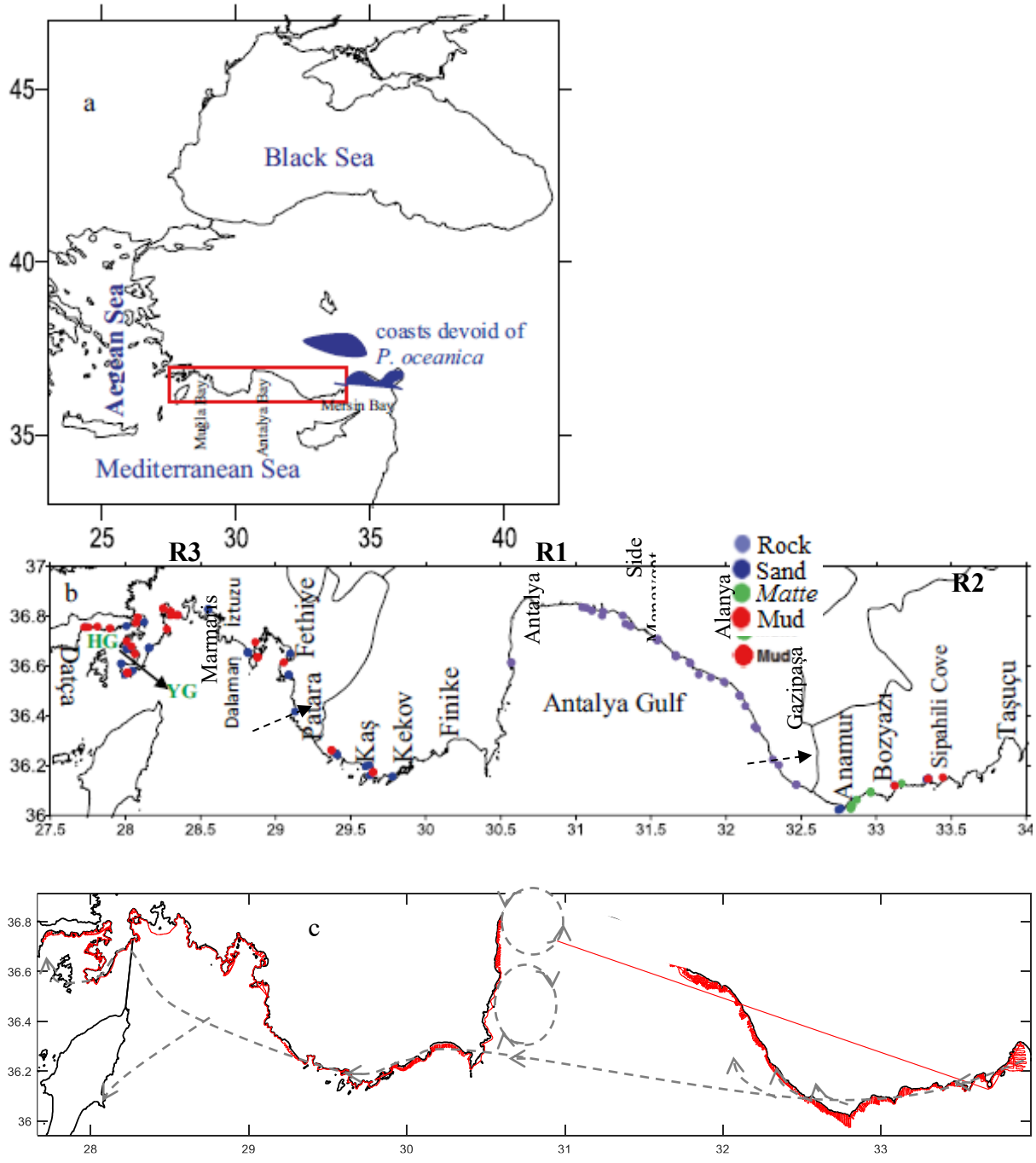

 doi:10.20944/preprints202603.1020.v1

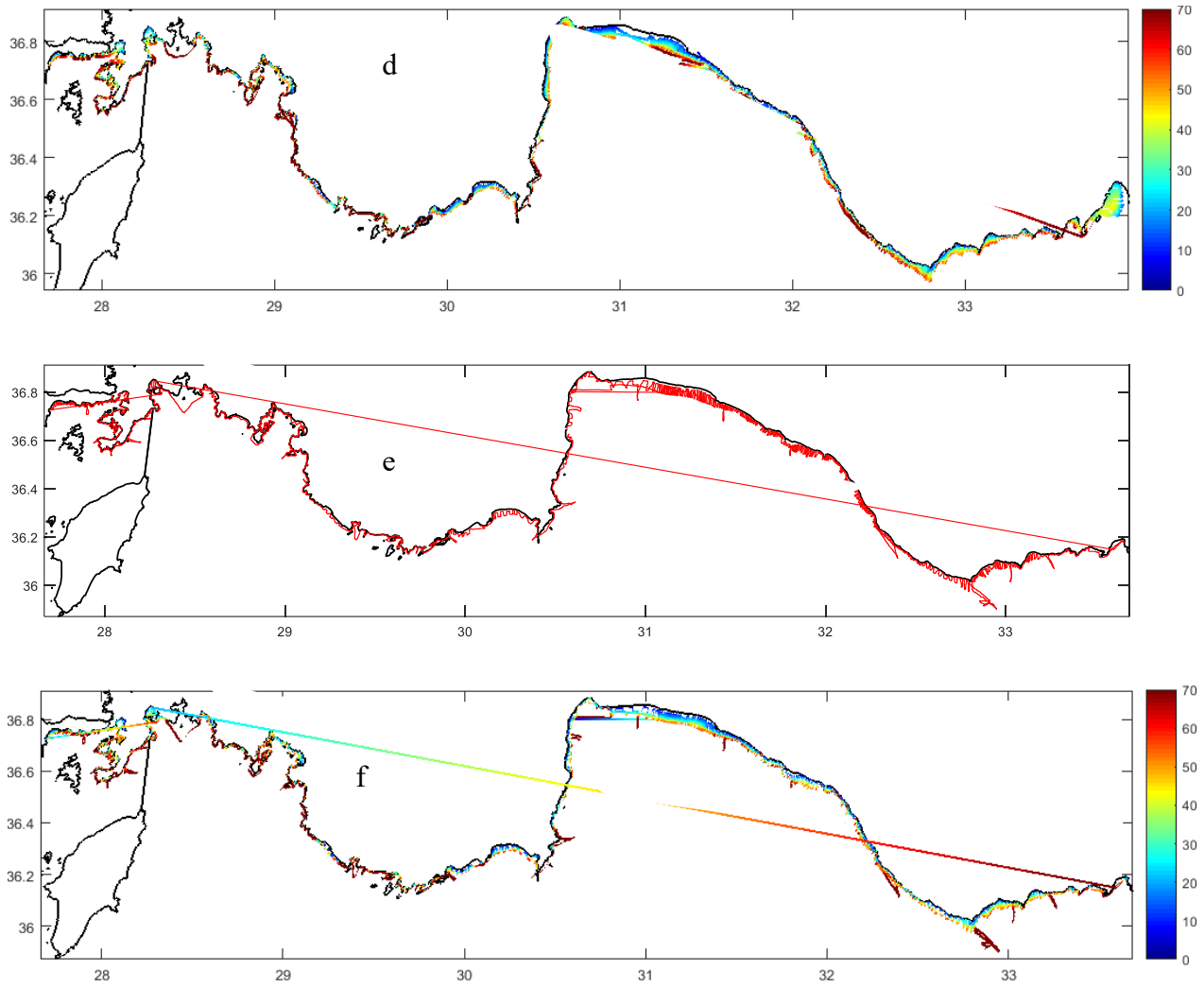

Figure 1. Study area in red rectangular and regions (R1-R3, dashed-line arrow shows border of the regions), bays (a, b), bottom types estimated by SCUBA (b), SCUBA sampling stations (YG is Yeşilova Gulf, and HG is Hisarönü Gulf, from Mutlu et al., 2023a), acoustical sampling tracklines (c, e) and rim water current and anti- and cyclonic current (c) and corrected bottom depths in meters by POSIBIOM (d, f) for. *P. oceanica* study conducted in winter and summer 2019, respectively.

2.2.2. Water Masses

Water masses showed a clear east–west trend in both winter and summer (Figure 2). In winter, waters from Antalya to the easternmost border of the study area were relatively warmer, more saline, and denser in both surface and near-bottom layers compared with the western part (Figure 2a,c,e).

In contrast, during summer, Antalya Gulf was distinguished by a specific water mass characterized by warm, saline, and dense waters compared with other areas along the rim current, which exhibited more saline, colder, and less dense surface waters. Near-bottom waters were similarly differentiated, with Antalya Gulf displaying the warmest conditions. In winter, the gulf contained saline and temperate waters, whereas in summer it exhibited the warmest waters with similar salinity. In both seasons, bottom depth did not strongly influence near-bottom physical characteristics, as maximum depths were limited to 35 m (Figure 2e,f). In winter, sea surface convection appeared toward the gulf around Anamur (Figure 1, 2).

2.2.3. Water Chemistry

Nutrient measurements were conducted only in summer. The highest average NO_2 + NO_3 concentrations were recorded in region 2, followed by regions 3 and 1. Concentrations varied

 doi:10.20944/preprints202603.1020.v1

between 2.17 and 2.69 mg L^{-1} in surface waters and between 1.64 and 1.87 mg L^{-1} in near-bottom waters. Surface PO_4 and SiO_2 concentrations increased slightly and markedly from west to east, respectively, in contrast to NH_4, which showed an opposite trend. Near-bottom PO_4 concentrations were highest in region 2 (9.61 mg L^{-1}) and lowest in region 1 (6.34 mg L^{-1}). Near-bottom SiO_2 concentrations ranged from 27.2 mg L^{-1} in region 2 to 37.4 mg L^{-1} in region 3. Maximum NH_4 concentrations were measured in region 3, whereas minimum values occurred in region 1.

Total suspended matter, measured only in summer, reached maximum (0.085 mg L^{-1}) and minimum (0.045 mg L^{-1}) values in region 3. Sea surface chlorophyll-a was lowest in region 2 (0.53 µg L^{-1}) and approximately doubled in region 1 (1.12 µg L^{-1}).

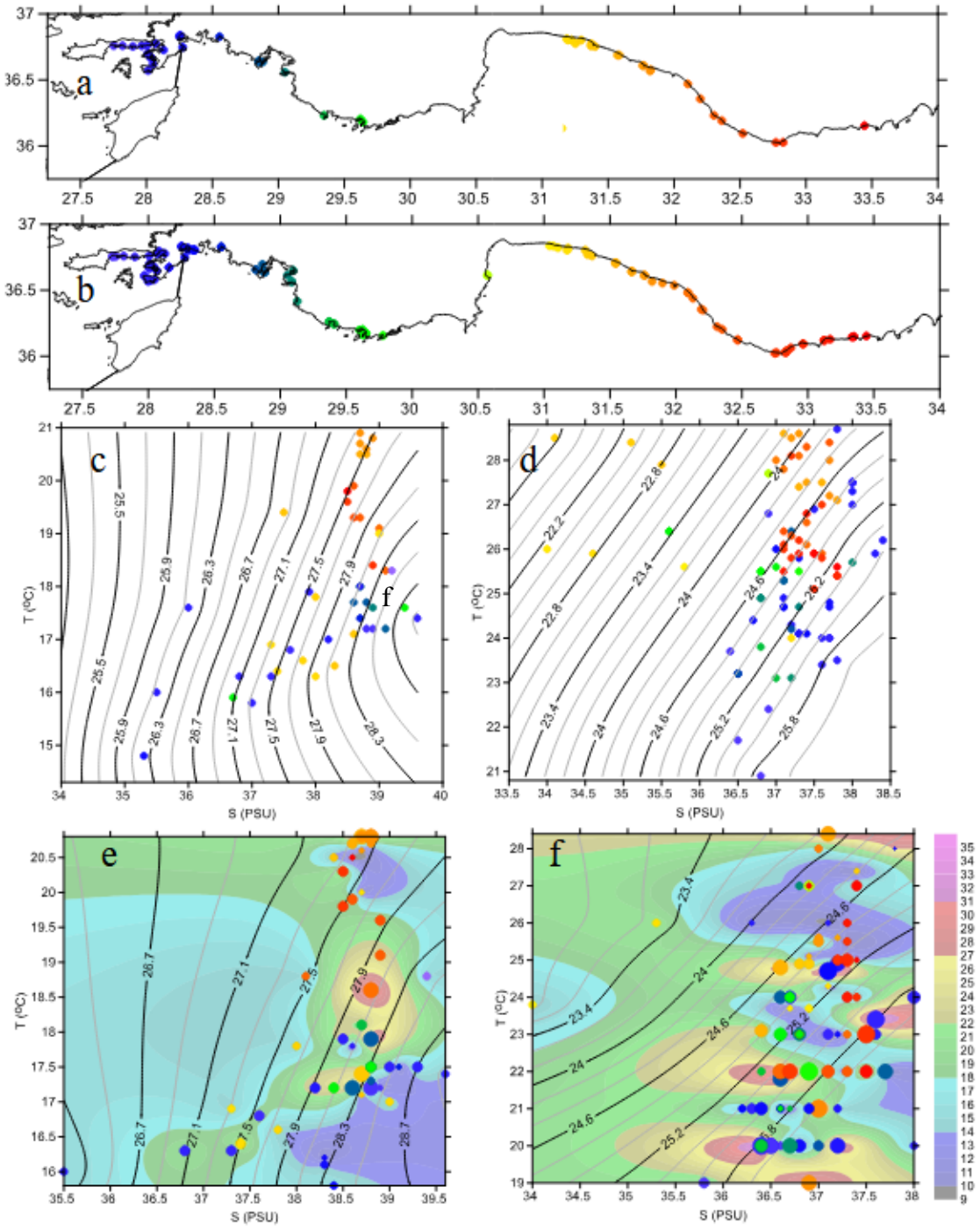

 doi:10.20944/preprints202603.1020.v1

Figure 2. SCUBA sampling stations colored with geographical coordinates in winter (a) and in summer (b), sea surface T-S diagram with water density contours, σ_t in winter (c) and summer (d), and near-bottom water T-S diagram in winter (e) and summer (f) with the bottom depth colored contours with color scale bar. Circles denote the bottom depth proportional to maximum depth of 35 m and colored with geographical coordinates in a and b, respectively.

2.2.4. Water Optics

Among optical variables, Secchi depth generally increased from east to west, particularly in summer, partly contrasting with %PAR. Secchi depth ranged between 3 and 29.5 m in winter and between 4 and 32 m in summer. Maximum PAR reaching the bottom was estimated at 30%, while average PAR values were approximately 3.07% in region 2 and 3.95% in region 3. The average depth corresponding to the minimum of the exponential attenuation curve was greatest in region 1 (KD: 10.69 ± 3.20 m), followed by region 3 (8.81 ± 3.36 m), and lowest in region 2 (6.88 ± 3.77 m).

2.2.5. General Characteristics

Based on Principal Component Analysis (PCA), the study area was primarily influenced by the first component, consisting of water temperature, oxygen, and pH in both seasons, with pH being more pronounced in summer. Seafloor depth represented the second component in both winter and summer, while Secchi depth was also an important variable of the second component in summer. Together, these variables explained approximately half of the spatial and seasonal environmental variance. Regions 1 and 2 were generally more saline and temperate than region 3, although salinity alone did not significantly explain seasonal or spatial differences. Considering only chemical parameters in summer, the study area was primarily structured by near-bottom nutrients, followed by surface-water N- and Si-based nutrients, total suspended matter, and chlorophyll-a.

2.2. Acoustical Sampling

Acoustical sampling was conducted using a quantitative scientific split-beam echosounder operating at 206 kHz during winter and summer 2019 along the entire Turkish Mediterranean coast. Approximately 2000 nautical miles were surveyed in each season. Tracklines were primarily oriented parallel to the coastline, with horizontal spacing of 300–500 m, extending from nearshore to a maximum depth of 70 m and offshore distances of 400–1000 m (Figure 1). Echosounder configuration and operational settings are provided in Table 1. A 0.1 ms signal was transmitted at 5 pings s^{-1} following calibration with a standard tungsten sphere using a pulse width of 0.4 ms. Surveys were conducted aboard R/V *Akdeniz Su* at a maximum speed of 5 knots. Data acquisition was performed using Visual Acquisition 6 (v6.3.1.10980, BioSonics Inc.), and files were stored in 30-min intervals.

Table 1. The configuration parameters of the digital echo sounder and settings during the data collection.

Echosounder parameters	**Values**
Manufacturer and model	BioSonics (USA) and DT-X
Acoustic frequency	206 kHz
Transducer type and shape	Split and circle
Source level	220.4 dB re µPa at 1 m
Receive sensitivity, narrow-beam	-51.0 dB re counts per µPa
Receive sensitivity, wide-beam	-56.0 dB re counts per µPa
Beam width	6.8 x 6.8°
System noise floor	-140 dB
Echosounder settings	
Transducer draft	2.5 m from the surface water

 doi:10.20944/preprints202603.1020.v1

Ping rate	5 pings s^{-1}
Sound speed*	calculated by Visual Acquisition
Absorption coefficient*	calculated by Visual Acquisition
Data collection threshold	-140 dB
Pulse width	0.1 ms
Maximum depth	70 (to-250) m

*referring the water temperature, salinity and pH.

2.3. Data Analyses

Raw acoustic data were processed using Visual Analyzer (v4.3) to convert files to ASCII (*.csv) format, followed by application of the POSIBIOM package [49] to correct bottom detection, remove noise, interference, and reverberation, and identify *P. oceanica* leaf biomass and length (canopy height). Visual Analyzer converted raw data into ping-to-ping horizontal and count-to-count vertical matrices at a resolution of one-eighth of the pulse width. Subsequent POSIBIOM processing first ensured accurate bottom detection, correcting biases caused by strong scatterers and tracking inconsistencies [49], thereby separating bottom echoes from seagrass rhizomes. A dead zone was then estimated to remove inconsistent echoes within rhizome length. Spurious water-column echoes were eliminated using a modified signal-to-noise ratio. Rhizome position was fixed, leaf length was estimated to confirm *P. oceanica* targets, and strong scatterers such as fish were removed. Output matrices included geographic coordinates, bottom depth, dead zone thickness, leaf biomass, leaf length, and sampling month based on seasonal regression equations between EDSU and leaf biomass [49]. A limitation of POSIBIOM is that EDSU–biomass relationships were derived from seagrass collected at 15 m depth on rocky substrate [50]; ongoing work aims to establish relationships for additional depths and substrates [59].

2.4. Bottom Types and Habitats

To verify acoustically determined distribution patterns, bottom type and bathymetry were analysed to define depth boundaries of seagrass distribution. Visual Bottom Typer (VBT; BioSonics Inc.) was applied using bottom echo signals. The B4 Fractal Dimension Method was selected due to the fractal nature of seabed structure. Bottoms were acoustically classified as rock (code 1), sand (smooth, code 2; rough, code 3), and mud (smooth, code 4; rough, code 5) following calibration settings [12]. Additionally, Visual Aquatic software, integrating VBT and EcoSAV, was used to estimate percent coverage and canopy height of submerged vegetation to further distinguish seagrass meadows from other macrophytes.

2.5. Conversion of Biomass to Biometrics

A total of 47 winter and 110 summer SCUBA samples were analysed for biometric characterization [12, 60]. Measured parameters included shoot density, leaf length, width, weight, biomass, inter-shoot distance, rhizome length and width, and number of leaves per shoot. These measurements were used to generate seasonal conversion equations linking acoustically estimated biomass to leaf area index, shoot density, and number of leaves. This approach enabled non-destructive estimation of multiple biometric parameters using acoustic data alone. The method was further applied at smaller spatial scales with monthly resolution in Antalya Gulf [58], providing additional conversion equations relevant to the present study.

2.6. Statistical Analyses

Conversion equations were tested for best-fit using t-tests for regression parameters (H_0: b = 0, a = 0) and correlation coefficients (H_0: r = 0). Analysis of covariance (ANCOVA) tested differences among regions, standard depth classes, and seasons (H_0: $S^2 = 0$).

 doi:10.20944/preprints202603.1020.v1

Spatial distributions of biometrics were mapped using kriging interpolation based on variogram analysis in SURFER 12 (Golden Software), with selected outputs transferred to QGIS. After testing normality using dispersion indices, four-way ANOVA was applied to evaluate differences among methods (acoustic vs SCUBA), seasons, bottom types, and depths, with additional one-way ANOVA and LSD post-hoc tests to identify factor-specific effects. Linear regression models (Estimated ~ 1 + Measured + Season + Bottom type + Depth) assessed relationships between estimated and measured biometrics and quantified the influence of each factor.

Multivariate analyses included PERMANOVA to test biometric differences between acoustic and SCUBA estimates across seasons, bottom types, and depths using PRIMER 6. After evaluating gradient lengths with detrended correspondence analysis, Canonical Correspondence Analysis (CCA) was applied to examine seagrass ecology in relation to environmental variables, with axis significance tested using Monte Carlo permutations (CANOCO v4.5). Non-metric multidimensional scaling (nMDS) was used to visualize inherent configuration of normalized biometric data, and RELATE analysis assessed correspondence between acoustic and SCUBA-based biometric resemblance matrices calculated using Euclidean distance. Statistical significance was accepted at $p < 0.05$.

3. Results

3.1. Acoustic–Biometrics Conversion

As a primary estimator, the POSIBIOM script [49] identifies *Posidonia oceanica* and estimates leaf length (m) and leaf biomass (g m^{-2}). To derive additional biometric parameters of the seagrass meadow, a set of biomass–biometric conversion relationships was previously established during 2011–2012 [58] (Table S1) and further refined in 2019 in the present study (Figure 3), with the exception of the biomass–number of leaves per shoot relationship, which was derived exclusively from SCUBA samplings.

Mutlu et al. (58 2026) established significant relationships between biomass and leaf area index (LAI), as well as shoot density, whereas the present study additionally examined the biomass–number of leaves relationship, although no significant correlation was detected (Table S1; Figure 3). For each period, biomass exhibited significant relationships with the other biometric parameters, with statistically significant differences observed among months and between seasons ($p < 0.05$). Accordingly, seasonal variability was explicitly incorporated into biomass-based biometric estimations in the present study.

The acoustic energy–biometric relationships implemented in POSIBIOM were derived from *P. oceanica* specimens collected at a standard depth of 15 m during monthly experimental surveys [50]. This depth exhibited wide annual variability in biometric measurements and has been used to distinguish between shallow and deep meadow characteristics [14]. The present study demonstrated that acoustic energy–biometric relationships varied significantly among months; however, variations in acoustic scattering properties across different depths or spatial scales were not examined.

To address this limitation, an ongoing project is investigating seasonal and depth-related variability in the acoustic scattering properties of seagrasses and other macrophyte species in the Mediterranean and Aegean Seas [61]. These considerations represent acknowledged limitations of the present study.

 doi:10.20944/preprints202603.1020.v1

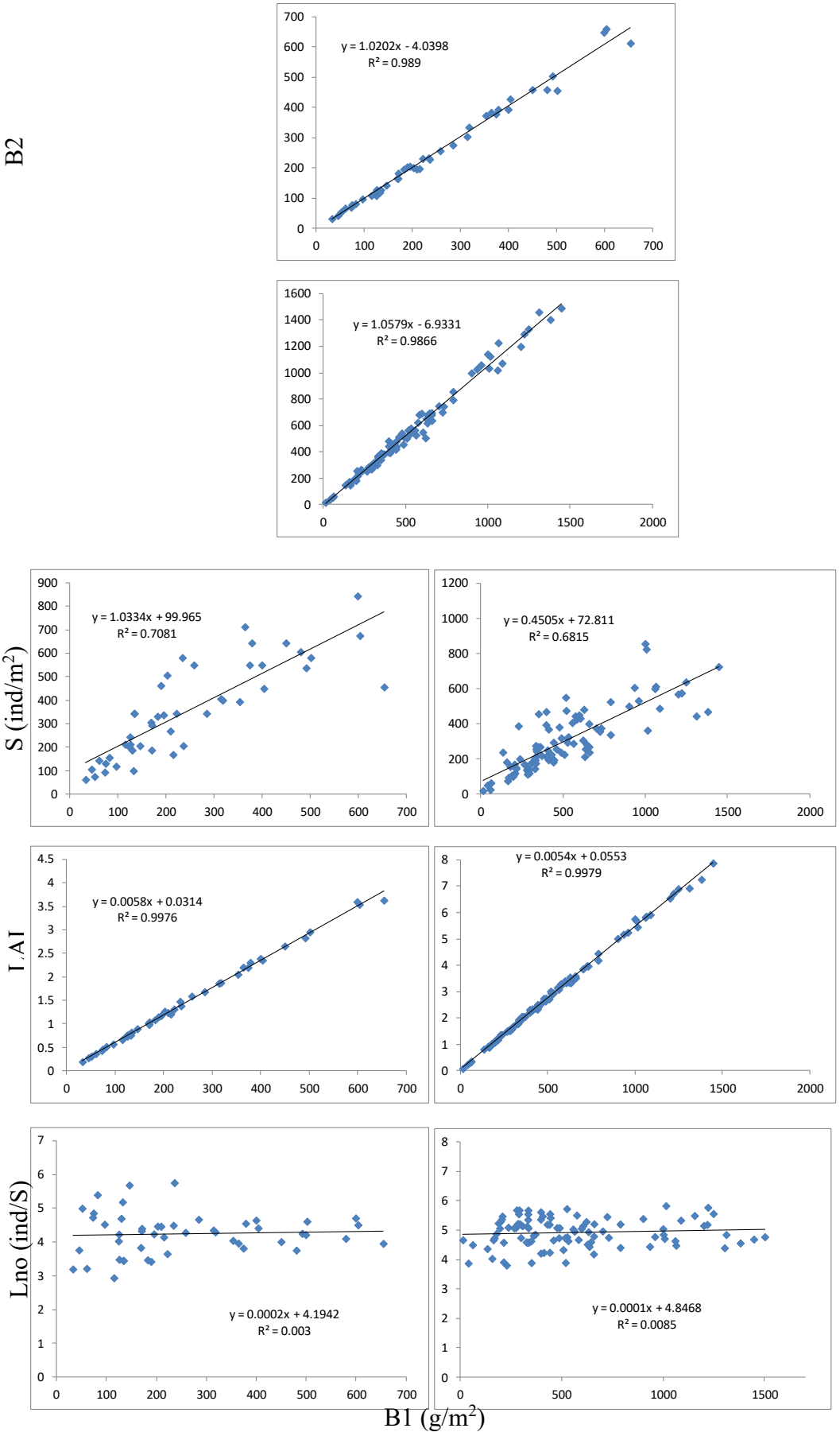

Figure 3. SCUBA-based biomass-other biometrics relation used as a conversion from acoustical biomass to LAI, shoot density, and number of leaf per shoot in winter (left panel) and summer (right panel). B1: leaf length- B2: leaf area-based-weight relation [12] for the biomasses.

 doi:10.20944/preprints202603.1020.v1

3.2. Spatio-Temporal Distribution

The total acoustically surveyed area was approximately 4,441.62 km² in winter and 4,934.33 km² in summer. The larger survey area in summer resulted from extended offshore transects conducted in conjunction with phytoplankton and zooplankton sampling activities (Figure 1).

3.2.1. Distribution and Coverage Area

The present study shows a bias toward winter acoustic data collection. During post-survey data evaluation, two sources of potential error were identified. First, the transducer was unintentionally tilted between Alanya and Anamur, which increased the apparent thickness of the bottom echo and may have led to misclassification of the signal as *Posidonia oceanica*. Second, between Antalya city centre and Serik, *Caulerpa prolifera* dominated the benthic vegetation and reached maximum canopy length during winter (November–March) [60, 62], causing POSIBIOM to classify some echoes as seagrass (Figures 4–5). Despite this limitation, POSIBIOM successfully detected *P. oceanica* within mixed vegetation assemblages where *C. prolifera* co-occurred. Ongoing work is addressing species-specific discrimination issues in acoustic detection [61]. Overall, *P. oceanica* was widely distributed in Antalya Gulf, where meadows occurred predominantly on rocky substrates, with limited occurrences on gravelly bottoms. Extensive and continuous meadows were observed between Serik and Side, where the gently sloping seafloor and wide continental shelf support broad habitat development (Figure 4). Secondary meadow areas were detected around Alanya, between Alanya and Anamur, and in the Marmaris and Datça bays.

The maximum depth limit of *P. oceanica* distribution ranged generally between 30 and 33 m across the study area, extending locally to 43 m in Fethiye Gulf (Figures 1, 4). Meadows occurred on a variety of substrates, including rocky bottoms in Antalya Gulf, matte substrates in Anamur and Bozyazı, and sandy to muddy bottoms throughout the remaining regions (Figures 1, 9). On hard substrates (rock and matte), *P. oceanica* could not be acoustically distinguished from the underlying bottom, consistent with findings from SCUBA-based observations reported by Mutlu et al. [14]. To address this limitation, bottom percent coverage estimates, presented later in the study, were used to refine and correct meadow occurrence in areas with ambiguous acoustic signals (Figure S6).

In terms of absolute meadow coverage, total *P. oceanica* area was estimated at 114.86 km² in winter and 96.27 km² in summer along the Turkish Mediterranean coast (Figure 4). The majority of coverage was concentrated in two major regions. Summer data provided a more accurate representation of meadow distribution, whereas overall coverage decreased from winter to summer (Figure 4). When excluding areas dominated by *C. prolifera* and *Cymodocea nodosa*, estimated *P. oceanica* coverage in winter decreased to 85.63 km² (Figure 4), indicating that winter distributions required additional correction to achieve accuracy comparable to summer observations.

 doi:10.20944/preprints202603.1020.v1

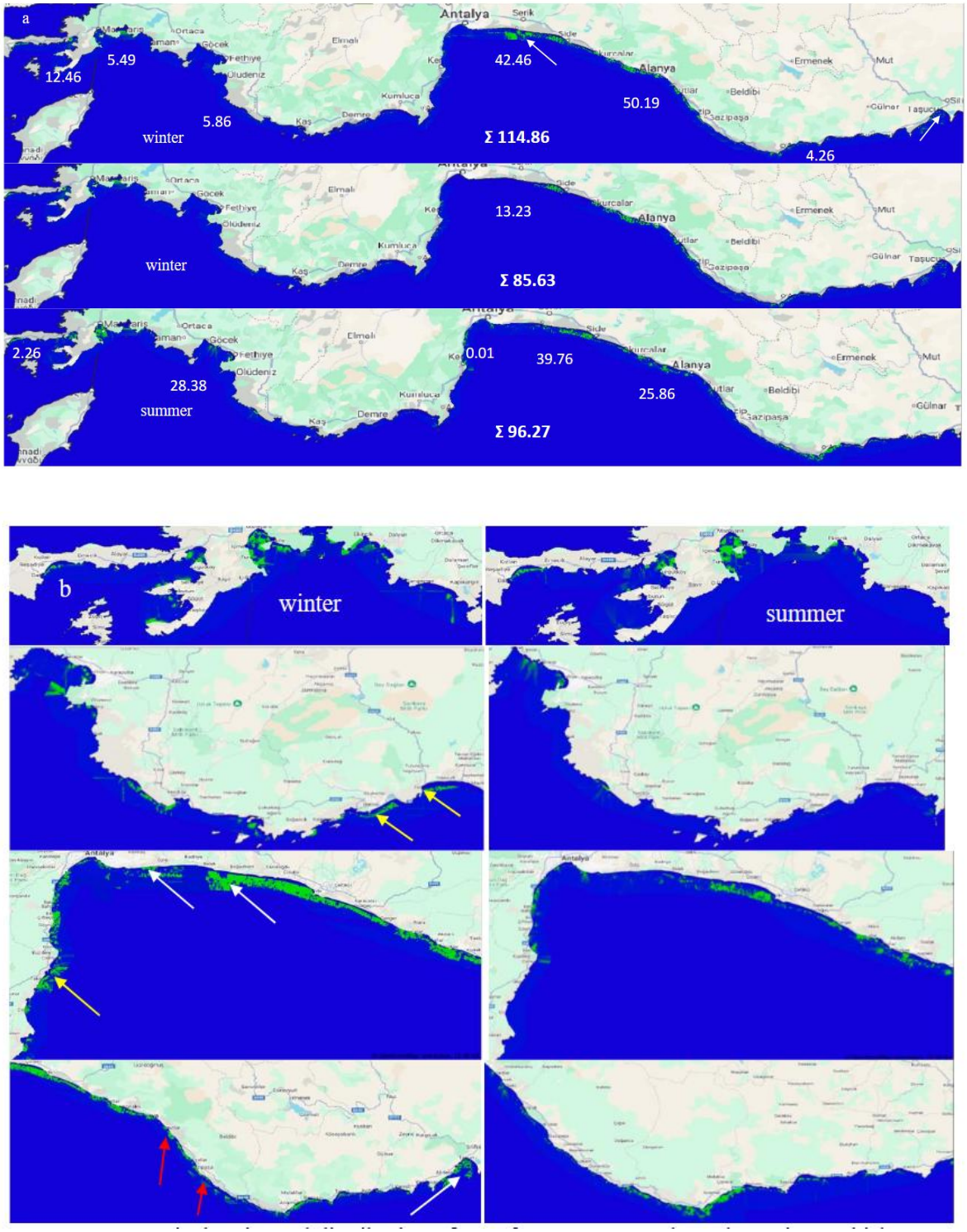

Figure 4. Acoustical-estimated distribution of *Posidonia oceanica* along the entire Turkish Mediterranean sea in winter and summer with regional and total area (km²) covered by *P. oceanica* and coverage area with excluded *Caulerapa prolifera* distribution in winter (a), and regional distribution for close-up view in winter (left panel) and summer (right panel) in direction of west to east of the study area (b). White arrow denotes *Caulerpa prolifera*, yellow *Cymodocea nodosa* and red a biased detection of *P. oceanica* due to the significantly tilted transducer.

3.2.2. Biometrical Distribution

Acoustically derived biometrics included leaf biomass (B1, g m^{-2}), leaf area index (LAI, m^2 m^{-2}), shoot density (S, ind. m^{-2}), and number of leaves per shoot (Lno, ind. $shoot^{-1}$). The measured biometric was leaf length, expressed as canopy height (L, m), reflecting the fact that *Posidonia oceanica*

 doi:10.20944/preprints202603.1020.v1

leaves exhibit variable orientations (flat, semi-erect, and erect) within the water column [12]. The study also compared biometrics obtained from acoustic estimates with those derived from SCUBA-based sampling. In SCUBA samples, leaf length represents the actual leaf size and does not correspond directly to canopy height, regardless of leaf orientation in situ. Results of the four-way ANOVA applied to all biometric variables are presented in Table 2. Significant differences were detected for each biometric between acoustic and SCUBA-based methods. These differences reflect methodological contrasts between indirect acoustic estimation and direct field measurements and are further evaluated in subsequent analyses.

Table 2. p values of 4-way ANOVA test (Method: M, Season: S, Bottom type: B, and Bottom depth: D) for differences in biometrics. Bold .value is significantly different at $p < 0.05$.

Source	d.f.	L	LAI	B1	S	Lno
M	1	**0.001**	**0.000**	**0.000**	**0.000**	0.103
S	1	**0.000**	**0.000**	**0.000**	**0.000**	**0.000**
B	3	**0.047**	**0.006**	**0.011**	**0.002**	**0.016**
D	6	0.089	**0.019**	**0.023**	0.070	**0.018**
M x S	1	**0.000**	**0.000**	**0.000**	**0.000**	0.258
M x B	3	**0.039**	**0.000**	**0.000**	**0.000**	**0.018**
M x D	5	0.064	**0.002**	**0.003**	**0.009**	**0.035**
S x B	3	0.766	0.122	0.170	0.223	0.519
S x D	3	0.867	0.525	0.425	0.489	0.693
B x D	15	0.743	0.921	0.953	1.000	0.794
M x S x B	3	0.224	0.879	0.896	0.045	0.513
M x S x D	3	0.685	0.565	0.440	0.597	0.599
M x B x D	14	0.834	0.920	0.961	0.976	0.711
S x B x D	6	0.690	0.886	0.912	0.837	0.236
M x S x B x D	6	0.743	0.767	0.773	0.887	0.285
Error	214					
Total	287					

Leaf Biomass, B1 (g m^{-2})

During spatial gridding to generate distribution maps, the averaging option in SURFER software was applied to measurements sharing identical interpolated geographical coordinates, reflecting temporal intervals of the D-GPS records. Consequently, Figure 5 presents average biomass distributions including zero-biomass values. For visualization purposes, maximum biomass values were truncated at 100 and 200 g m^{-2} to enhance the display of lower biomass ranges. Mean biomass values at non-zero locations were 603.8 ± 1.1 g m^{-2} in winter and 634.3 ± 0.9 g m^{-2} in summer (Figure 5). Using acoustic and SCUBA-based approaches, biomass ranged from 32.7–248.3 g m^{-2} and 172.7–1183.8 g m^{-2} in winter, and from 12.7–480.8 g m^{-2} and 290.1–905.0 g m^{-2} in summer, respectively. In winter, maximum biomass occurred in the Side meadow, whereas in summer, maxima were observed in both Side and Marmaris bays, followed by Anamur and Datça bays. This spatial pattern appeared to be associated with the occurrence of hard substrates and was more pronounced during summer (Figure 5). Biomass differed significantly among bottom types in both seasons; however, unlike summer, SCUBA-based biomass estimates did not vary significantly with bottom depth in winter (Table 3).

In winter, acoustically estimated biomass was lowest at 10 m depth, increased at 15 m, slightly decreased at 20 m, and reached its maximum at 30 m, with all depths being significantly differentiated

 doi:10.20944/preprints202603.1020.v1

from one another (Table 4; Figures 6, S1). Biomass was significantly lower on rocky and sandy bottoms compared to muddy substrates (Table 4; Figures 6, S2). In contrast, SCUBA-based biomass ranged between approximately 200 and 260 g m^{-2} and did not differ significantly among depths (Table 4; Figures 6, S1). Biomass values on sand, rock, and matte substrates were similar and significantly higher than those on muddy bottoms (Table 4; Figures 5, S2). Unlike winter, summer biomass showed significant differentiation by both bottom depth and substrate type for acoustic and SCUBA-based estimates (Table 4; Figures 7, S3, S4). Biomass trends were broadly consistent between methods: following relatively low values (with an exception at 5 m), biomass declined gradually from 10 to 25 m and then increased again at 30 m. Maximum biomass occurred at 10 m depth for both methods (Table 4; Figure 7). Biomass patterns across bottom types were also highly consistent between methods, with hard substrates supporting higher biomass and muddy substrates exhibiting the lowest values (Table 4; Figures 7, S4).

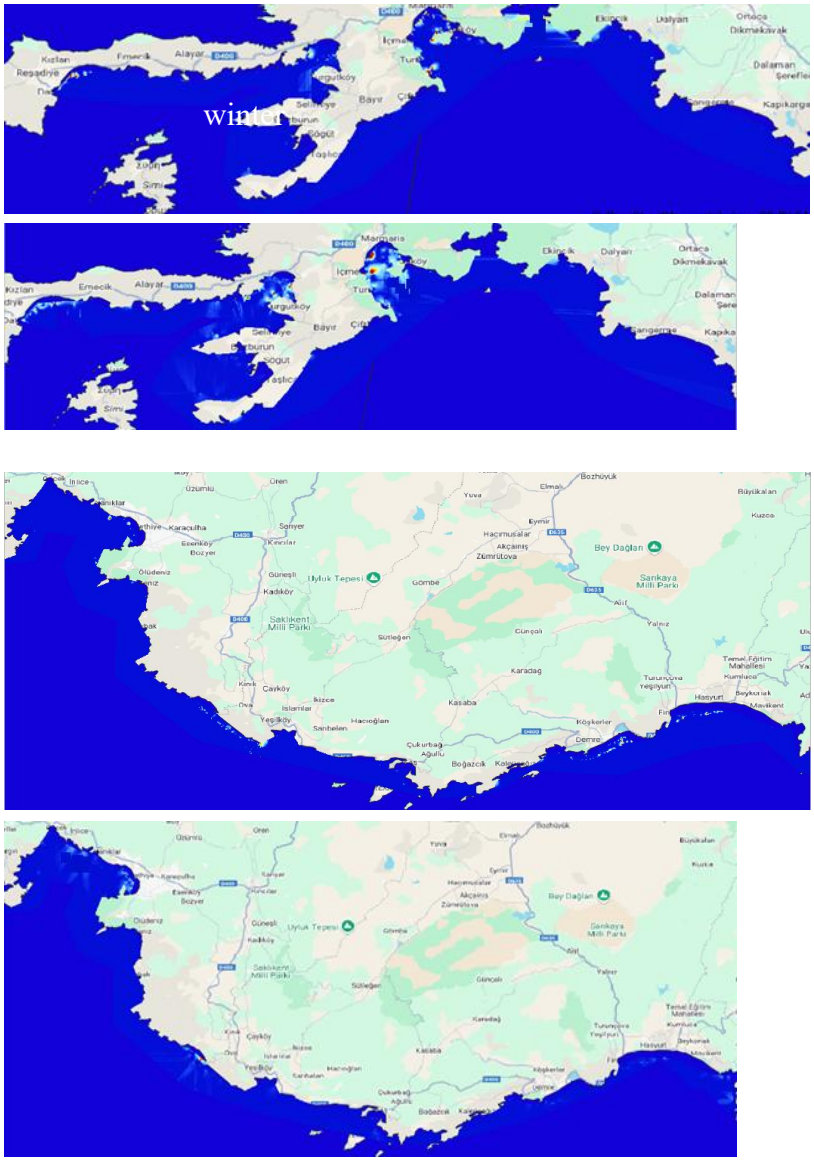

 doi:10.20944/preprints202603.1020.v1

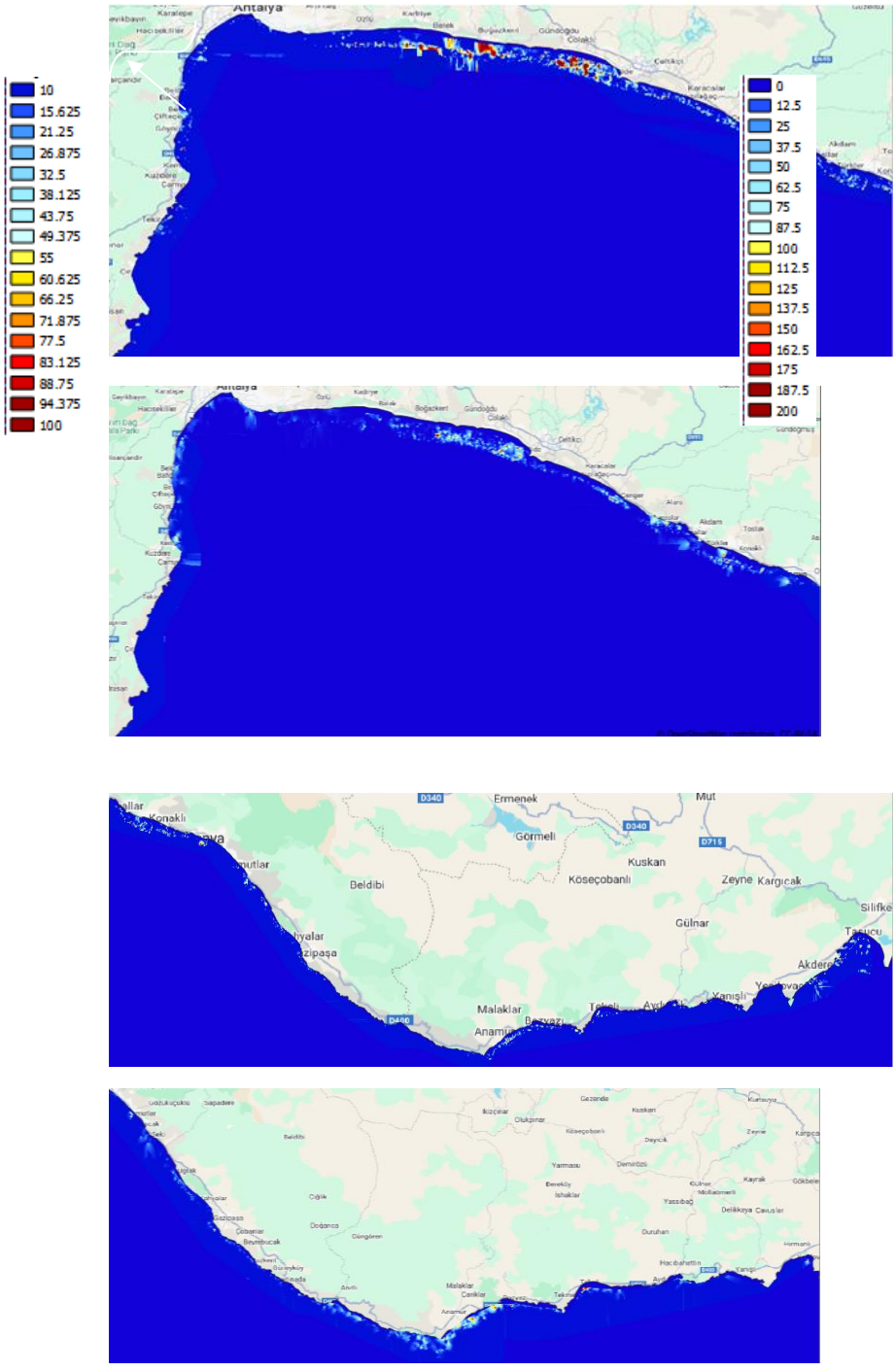

Figure 5. Regional leaf biomass (g/m²) distribution of *Posidonia oceanica* in winter (left panel) and summer (right panel) in direction of west to east of the study area. Arrow denotes *Caulerpa prolifera*.

A significant seasonal difference in biomass was detected for both methods (Table 3). Acoustic estimates indicated higher biomass in summer than in winter, accounting for approximately 97% of summer values, whereas SCUBA-based estimates showed nearly a twofold increase in summer relative to winter (Table 4; Figures 8, S5). Overall, biomass differed significantly among methods, seasons, bottom depths, and substrate types. Among interaction terms, only those involving the method factor significantly influenced biomass, whereas other interactions were not significant (Table 2).

 doi:10.20944/preprints202603.1020.v1

Table 3. p values of ANOVA test for differences in acoustically and SCUBA-wise estimated biometrics by bottom depths (D), and types (BT) in winter (W) and summer (S) and in seasons. Bold .value is significantly different at $p < 0.05$.

	Acoustics					SCUBA				
W	**L**	**LAI**	**B1**	**S**	**Lno**	**L**	**LAI**	**B1**	**S**	**Lno**
D	**0.000**	**0.000**	**0.000**	**0.000**	**0.000**	0.749	0.742	0.856	0.944	0.840
BT	**0.022**	**0.000**	**0.000**	**0.000**	**0.000**	**0.034**	0.057	**0.029**	**0.010**	0.504
S										
D	**0.000**	**0.000**	**0.000**	**0.000**	**0.000**	0.494	**0.011**	**0.034**	**0.001**	**0.012**
BT	**0.000**	**0.000**	**0.000**	**0.000**	**0.000**	0.087	**0.006**	**0.002**	**0.000**	**0.038**
Season	**0.000**	**0.000**	**0.000**	**0.000**	**0.000**	**0.000**	**0.000**	**0.000**	0.198	**0.000**

Leaf Area Index, LAI (m^2 leaf area m^{-2} Bottom Area)

Because *Posidonia oceanica* leaves have two surfaces, leaf area was estimated using one side only and is therefore expressed as one-sided leaf area. Similar to biomass, LAI differed significantly among methods, seasons, bottom depths, and substrate types. However, among interaction terms, only those involving the method factor were significant, whereas higher-order interactions (Method × Season × Bottom type × Depth) showed no significant effects (Table 2). One-way ANOVA indicated that LAI varied significantly with bottom depth and substrate type in summer for both acoustic and SCUBA-based estimates, whereas in winter no significant differences were detected by bottom depth or substrate type for SCUBA measurements (Table 3).

Mean LAI derived from acoustic estimates was 3.56 ± 0.01 in winter and 3.48 ± 0.01 in summer, whereas SCUBA-based estimates averaged 1.4 ± 0.2 and 3.1 ± 0.1 in winter and summer, respectively (Table 4; Figures 8, S5). Overall, LAI ranged from 0.1–1.5 to 10.0–6.9 in winter and from 0.1–2.7 to 15.3–4.9 in summer for acoustic and SCUBA methods, respectively. In winter, mean LAI was higher in acoustic estimates (3.56 ± 0.01) than in SCUBA measurements (1.4 ± 0.2). Acoustically estimated LAI showed an increasing trend with depth, whereas SCUBA-based LAI remained relatively constant across depths, ranging approximately between 1.1 and 1.5 and showing no significant depth-related differences. Across substrate types, LAI increased from rock to sand to mud and was significantly higher on sand than on both rock and mud substrates (Table 4; Figures 6, S1, S2). In summer, average LAI values were more similar between methods (3.48 ± 0.01 for acoustics and 3.1 ± 0.1 for SCUBA) than in winter. Acoustically derived LAI was significantly lower at 20 m compared to other depths, whereas SCUBA-based LAI was higher at 10–20 m than at greater depths. In both methods, non-mobile substrates supported higher LAI values than mobile substrates (Table 4; Figures 7, S3, S4).

 doi:10.20944/preprints202603.1020.v1

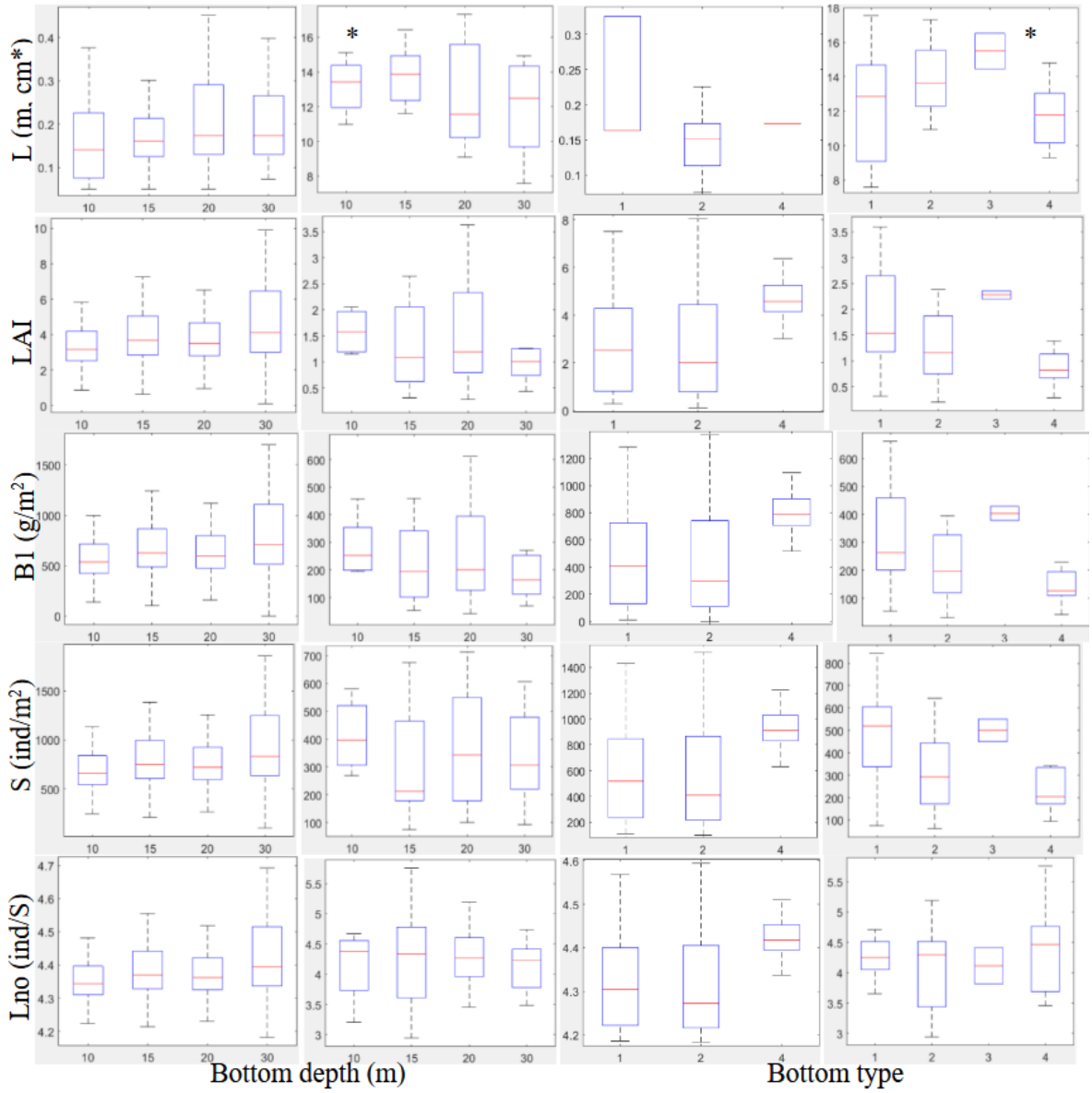

Figure 6. Box plot of the biometrics estimated from acoustic (left panel) and SCUBA (right panel) sampling by bottom depths and bottom types (1: rock, 2: sand, 3: *matte* and 4: mud), respectively in winter.

Shoot Density, S (ind. m^{-2})

Seasonal mean shoot density was higher in winter than in summer for both acoustic and SCUBA-based methods. Mean values ranged from 723.3 ± 1.0 ind. m^{-2} in winter to 359.7 ± 27.7 ind. m^{-2} in summer for acoustic estimates, and from 358.5 ± 0.8 ind. m^{-2} in winter to 316.1 ± 19.2 ind. m^{-2} in summer for SCUBA measurements (Tables 3–4; Figures 7, S5). A statistically significant seasonal difference was detected only for acoustic estimates (Table 3; Figure S5). Maximum shoot density values reached 1884.8 and 1323.3 ind. m^{-2} in winter and 1093.8 and 480 ind. m^{-2} in summer for acoustic and SCUBA-based methods, respectively. Minimum values ranged from 99.9 to 356.6 ind. m^{-2} in winter and from 18.8 to 289.4 ind. m^{-2} in summer for the respective methods.

Shoot density differed significantly among methods, seasons, bottom depths, and substrate types. Among interaction terms, only those involving the method factor significantly affected shoot density, with the exception of the Method × Depth interaction; all higher-order interactions were not significant (Table 2). Similar to LAI, shoot density patterns across bottom depths and substrate types were broadly consistent between acoustic and SCUBA-based estimates in both seasons. In both winter and summer, soft (mobile) substrates supported significantly higher shoot densities than non-

 doi:10.20944/preprints202603.1020.v1

mobile substrates, in contrast to biomass patterns (Figures 6–7, S1–S4). Acoustically derived shoot density was significantly lower at 20 m compared to other depths, whereas SCUBA-based estimates indicated higher shoot densities at 10–20 m relative to greater depths, but only during summer.

Table 4. Bottom depth and type wise distribution of mean value ± SD at 95% confidence of the biometrics estimated from acoustic and SCUBA sampling in winter and summer, and seasonal distribution. * Length is in meter.

	Acoustics					SCUBA				
Winter	**L***	**LAI**	**B1**	**S**	**Lno**	**L**	**LAI**	**B1**	**S**	**Lno**
D										
10	0.17±0.01	3.5±0.1	594.3±6.5	713.2±6.7	4.3±0.1	13.1±1.1	1.5±0.3	262.7±60.0	386.7±72.0	4.1±0.2
15	0.18±0.01	3.9±0.1	671.6±4.7	793.2±4.9	4.3±0.1	13.5±0.9	1.4±0.2	255.4±47.0	340.3±56.5	4.2±0.1
20	0.22±0.01	3.7±0.1	636.1±4.3	757.7±4.4	4.3±0.1	13.3±0.7	1.5±0.2	262.3±37.9	369.0±45.5	4.3±0.1
30	0.20±0.01	4.3±0.1	750.4±6.8	878.8±7.1	4.4±0.1	11.9±1.2	1.1±0.3	200.1±64.1	338.3±77.0	4.1±0.2
BT										
1	0.23±0.01	2.8±0.1	485.8±6.9	601.5±7.1	4.3±0.1	12.4±0.7	1.8±0.2	315.6±36.4	462.1±42.5	4.3±0.1
2	0.17±0.01	2.8±0.1	456.4±10.6	571.8±10.9	4.3±0.1	14.8±0.7	1.3±0.2	234.2±39.9	309.5±46.5	4.1±0.1
3						15.4±2.1	2.2±0.6	402.9±109.4	500±127.5	4.1±0.4
4	0.21±0.01	4.8±0.1	823.6±9.6	950.6±9.9	4.4±0.1	11.7±0.8	0.9±0.2	159.2±42.9	254.3±50.0	4.3±0.1
Summer										
D										
5						21.4±6.6	3.5±2.0	650.9±432.3	481.2±174.6	4.5±0.5
10	0.17±0.01	3.5±0.1	642.0±3.6	362.0±1.6	4.9±2.9 e-4	26.3±1.5	4.1±0.4	782.9±99.1	417.1±40.1	4.6±0.1
15	0.17±0.01	3.5±0.1	638.2±2.0	360.3±0.9	4.9±1.6 e-4	24.7±1.3	3.3±0.4	637.9±90.1	353.5±36.4	5.0±0.1
20	0.19±0.01	3.3±0.1	615.1±2.0	349.9±0.9	4.9±1.6 e-4	27.1±1.4	3.6±0.4	664.2±92.1	348.0±37.2	4.9±0.1
25	0.19±0.01	3.5±0.1	639.2±2.4	360.7±1.1	4.9±1.9 e-4	25.0±1.7	2.2±0.5	416.0±111.6	217.5±45.1	5.3±0.1
30	0.15±0.01	3.4±0.1	635.4±2.2	359.0±1.0	4.9±1.8 e-4	25.0±1.8	2.2±0.5	421.2±119.9	250.0±48.4	4.8±0.1

 doi:10.20944/preprints202603.1020.v1

35						21.1±2.5	1.2±0.7	216.5±163.4	129.4±66.0	4.9±0.1
BT										
1	0.21±0.01	4.1±0.1	742.7±8.9	407.3±4.1	4.9±7e-4	23.6±1.33	3.9±0.4	775.1±86.7	427.8±35.2	5.1±0.1
2	0.13±0.01	3.3±0.1	603.1±2.3	344.4±1.1	4.9±1e-4	24.8±1.0	2.8±0.3	520.4±68.9	293.9±28.0	4.8±0.1
3	0.21±0.01	3.6±0.1	663.3±11.3	371.3±5.1	4.9±9e-4	30.3±2.3	4.6±0.7	906.2±150.2	436.7±61.0	4.6±0.1
4	0.23±0.01	3.5±0.1	652.2±3.8	366.6±1.7	4.9±3e-4	26.0±1.1	2.3±0.3	413.8±77.5	222.7±31.5	4.9±0.1
Seaason										
1	0.20±4.3e-4	3.56±0.01	603.8±1.1	723.3±1.0	4.3±3.1e-4	13.1±0.8	1.4±0.2	251.4±55.1	359.7±27.7	4.2±0.1
7	0.18±3.7e-4	3.48±0.01	634.3±0.9	358.5±0.8	4.9±2.9e-4	25.3±0.5	3.1±0.1	580.4±38.2	316.1±19.2	4.9±0.1

Number of Leaves per Shoot, Lno (ind. Shoot^{-1})

Although regression equations between biomass and number of leaves per shoot were not statistically significant, the data points did not exhibit a circular or random scatter pattern. This reflects the relatively narrow range of mean Lno values, which varied between 3.8 and 6.7 across both seasons and methods. Lower biomass values were associated with higher and more variable Lno estimates (Figure 3).

Seasonal mean Lno values ranged from 4.3 ± 3.1 × 10^{-4} to 4.9 ± 2.9 × 10^{-4} ind. shoot^{-1} for acoustic estimates and from 4.2 ± 0.1 to 4.9 ± 0.1 ind. shoot^{-1} for SCUBA-based measurements (Figures 8, S5). No significant differences in Lno were detected between methods, whereas significant differences were observed among seasons, bottom depths, and substrate types (Table 2). The Method × Season interaction was not significant, while other interactions involving the method factor significantly influenced Lno. In summer, Lno values were higher on rocky substrates compared to other bottom types, in contrast to winter patterns (Figures 6–7, S2, S4). A depth-related trend in Lno was observed; however, this trend was not statistically significant (Figures 6–7, S1, S3).

 doi:10.20944/preprints202603.1020.v1

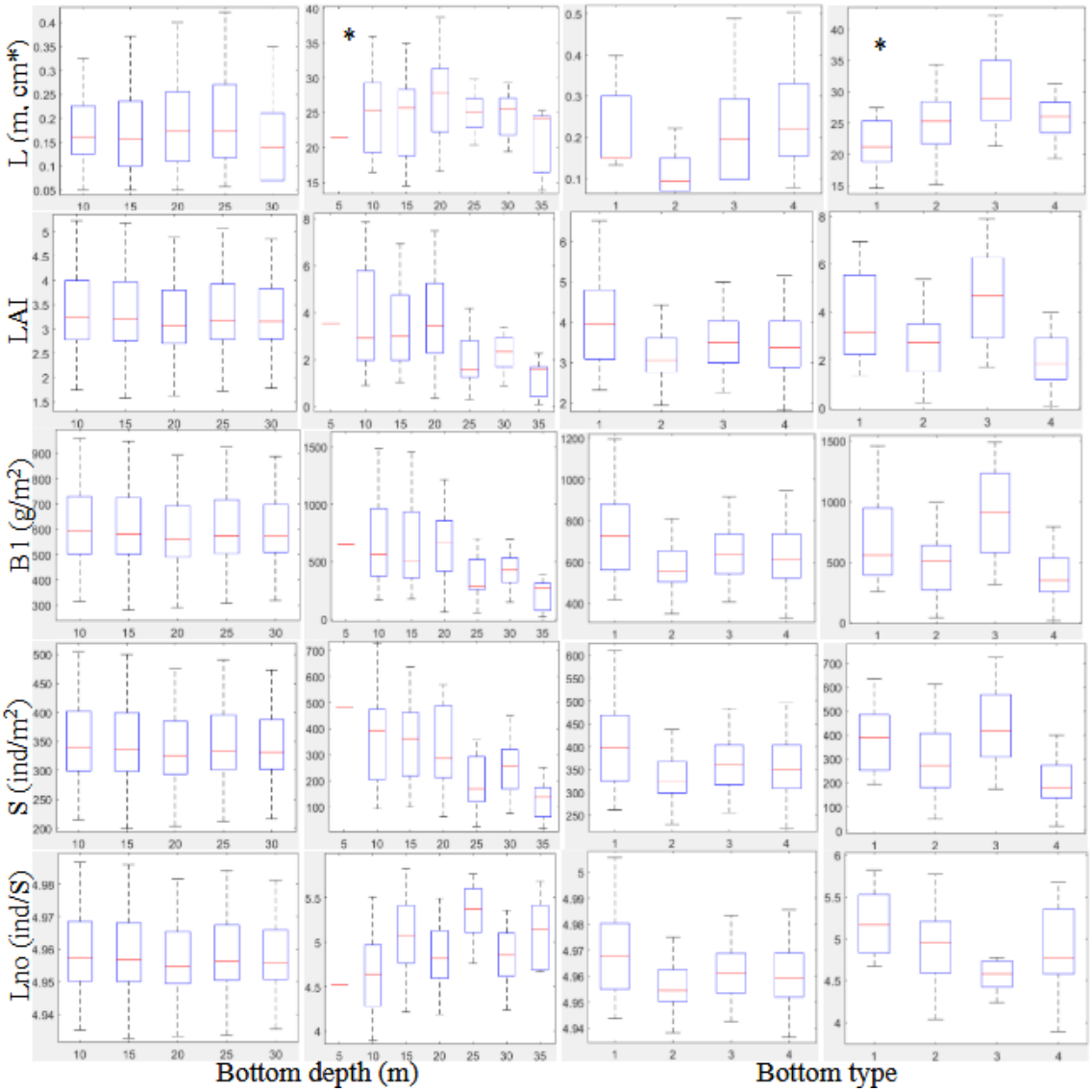

Figure 7. Box plot of the biometrics estimated from acoustic (left panel) and SCUBA (right panel) sampling by bottom depths and bottom types (1: rock, 2: sand, 3: *matte* and 4: mud), respectively in summer.

Leaf Length, L (cm)

Leaf length was measured *ex situ* from SCUBA samples without considering leaf orientation, whereas acoustic estimates were obtained *in situ* and reflect the natural orientation of leaves above the seafloor. Consequently, acoustically derived leaf length represents canopy height and is expected to be shorter than the true leaf length measured from SCUBA samples.

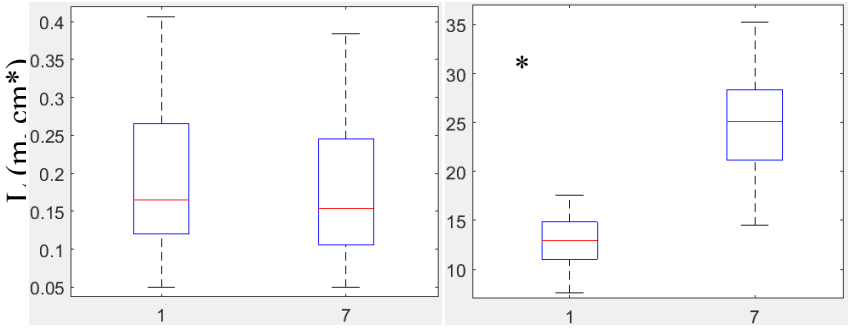

 doi:10.20944/preprints202603.1020.v1

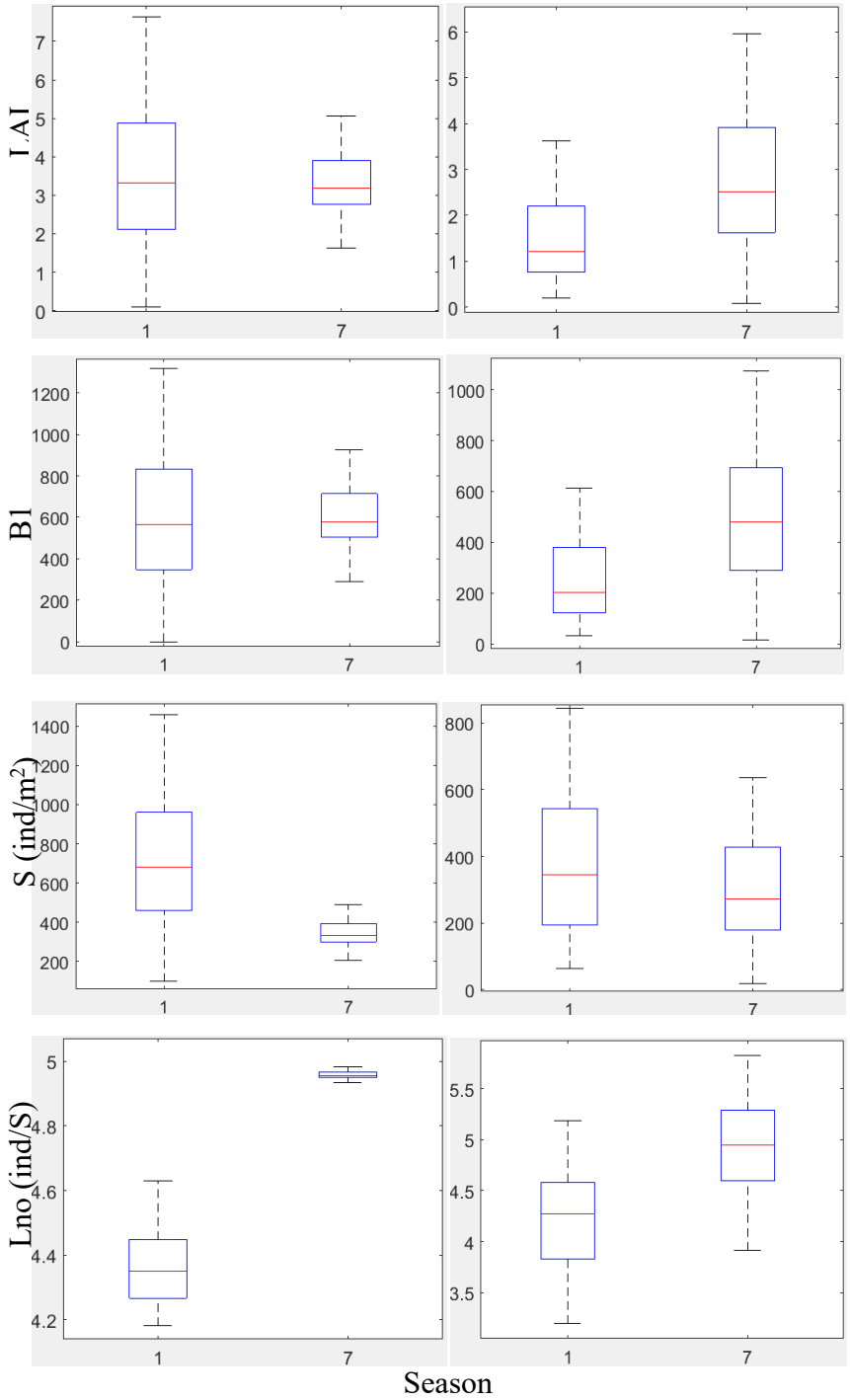

Figure 8. Box plot of the biometrics estimated from acoustic (left panel) and SCUBA (right panel) sampling by season (1: winter and 7: summer).

Leaf length differed significantly among methods, seasons, and substrate types, whereas no significant differences were detected among bottom depths or for the Method × Depth interaction. Other interaction terms involving the method factor significantly affected leaf length (Table 2). One-way ANOVA indicated that acoustically estimated leaf length differed significantly among depths, substrate types, and seasons in both winter and summer, whereas SCUBA-based leaf length varied only by substrate type in winter and between seasons (Table 3; Figures 6–8, S1–S5).

Minimum and maximum leaf length values ranged from 5.0–13.8 cm and 70.0–29.7 cm in winter, and from 11.3–11.8 cm and 49.5–27.3 cm in summer, for acoustic and SCUBA-based estimates, respectively. Seasonal mean leaf length varied between 20.0 ± 4.3 × 10^{-2} cm in winter and 18.0 ± 3.7 × 10^{-2} cm in summer for acoustic estimates, and between 13.1 ± 0.8 cm and 25.3 ± 0.5 cm for SCUBA measurements (Table 4; Figures 8, S5). Seasonal patterns differed between methods, with acoustically

 doi:10.20944/preprints202603.1020.v1

derived canopy height being higher in winter than in summer, whereas SCUBA-based leaf length was higher in summer than in winter. Based on acoustic estimates, leaf length increased from 10 to 20 m depth and then decreased at 30 m, whereas no significant depth-related trend was observed in SCUBA measurements during winter. Regarding substrate type, rocky bottoms supported the greatest canopy height in acoustic estimates, whereas in SCUBA measurements leaf length was greater on sand than on rock, followed by mud substrates during winter (Table 4; Figures 6, S1–S2). In summer, depth-related patterns were similar to those observed in winter. Acoustically derived leaf length was higher on hard substrates than on sand but lower than on mud, whereas SCUBA measurements indicated higher leaf length only on matte substrates compared to rock and sand (Table 4; Figures 7, S3–S4).

Furthermore, Visual Aquatic was used to estimate percent coverage and plant height in order to compare these data with those obtained in the present study (Figures S6, S7). Detection of *P. oceanica* functioned well using POSIBIOM, in contrast to the Visual Aquatic estimates, which indicated 100% bottom coverage by the plant in both winter and summer. This resulted in a biased detection in a specific area during winter, when the transducer was significantly tilted (Figure S6). Other macrophytes covered less than 20% of the bottom in both seasons.

3.2.3. Habitats

Habitat characterization consisted of analyses of bottom types and sediment thickness (Figures 9, S8). For this purpose, the software VBT (BioSonics Inc.), which was later upgraded and integrated into ECOSAV and subsequently into Visual Habitat and Visual Aquatic (BioSonics Inc.), was employed. The latter two software packages apply different solution methods that are difficult to calibrate with *in situ* sedimentary characteristics of the seabed, unlike VBT. VBT allows calibration for different bottom types and sediment compositions, as demonstrated by Mutlu et al. [12] along the Antalya Gulf coast. Although VBT has been out of use for several years, it was preferred in the present study due to its calibration capability.

Bottom Types

Bottom types were classified into five categories: slime sand, rough sand (>70% content), slime mud, rough mud (>70%), and rock/*P. oceanica* (Figure 9). The acoustic hardness of rock and *P. oceanica* was similar because the seagrass formed a dense distribution, with coverage close to 100% of the bottom, as estimated by Visual Aquatic [12].

Between Anamur and Taşucu Bay, an area influenced by the Göksu River delta and outflow near Taşucu and by the westerly rim current (Figure 1), coarse sand was absent and replaced by slime sand, with the exception of rough sand observed in Akkuyu Bay. In summer, rock/seagrass bottoms were present, and from Anamur eastward to Bozyazı the bottom was predominantly matte covered by seagrass meadows. Further east, the bottom consisted mainly of mobile substrates (Figure 9). Between Anamur and Alanya, the continental shelf was narrow, and shallow bottoms were dominated by rough sand, with partial coverage of rough mud and small seagrass patches. In winter, a significantly tilted transducer position increased the thickness of the bottom echo, leading to misclassification by the commercial software (Figure 9). After recognizing this issue, the transducer was repositioned perpendicular to the seabed, resulting in more reliable bottom-type identification, particularly in summer for this area. Between Alanya and the Antalya city center, where the continental shelf is widest within the study area, bottom types were distributed along a depth gradient from the coast to offshore waters, transitioning from rough sand to slime sand, rough mud, and slime mud (Figure 8). *P. oceanica* beds were more extensive in this region than elsewhere along the Turkish Mediterranean coast. The spatial extent of these beds was more pronounced in winter than in summer, when bed coverage was comparatively reduced (Figure 9). In contrast, *P. oceanica* was reported to inhabit only rocky substrates in the Antalya Gulf (from Anamur to Cape Finike) [14]. A similar distribution pattern was observed between Finike and Kekova, although with a lesser westward extent. West of this region, sand fractions were largely absent and mud fractions

 doi:10.20944/preprints202603.1020.v1

predominated. Some acoustic detections of seagrass were recorded, and Mutlu et al. [14] classified this area as mobile substrate with seagrass occurrence. Exceptions to this general pattern were noted, as rough sandy bottoms occurred locally in shallow areas within gulfs such as Fethiye, Marmaris, and Hisarönü (Figure 9).

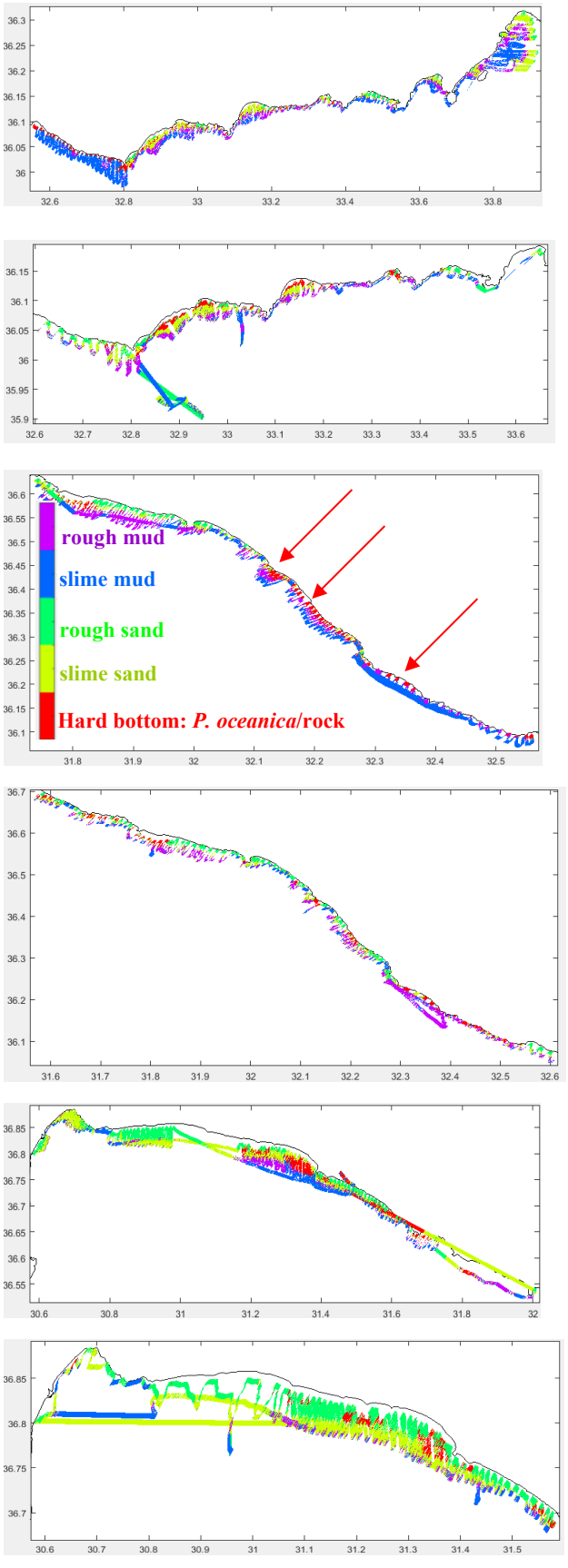

 doi:10.20944/preprints202603.1020.v1

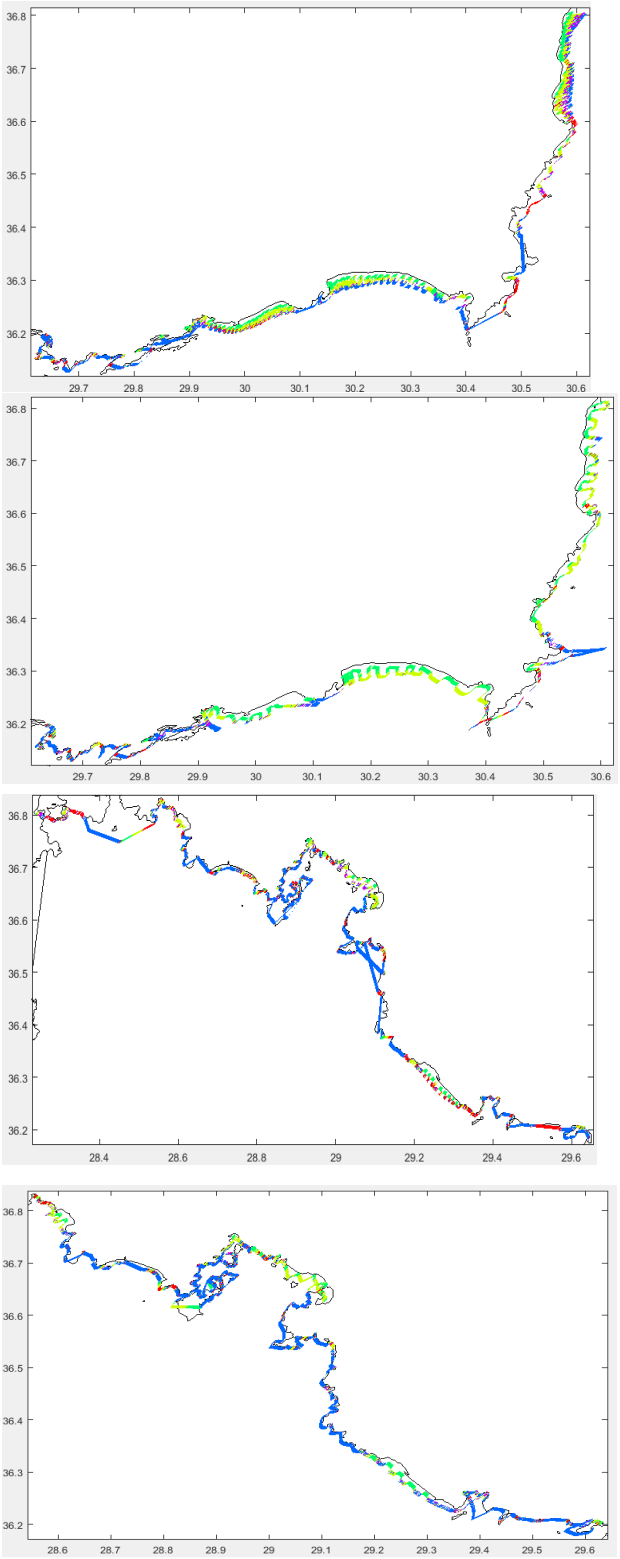

 doi:10.20944/preprints202603.1020.v1

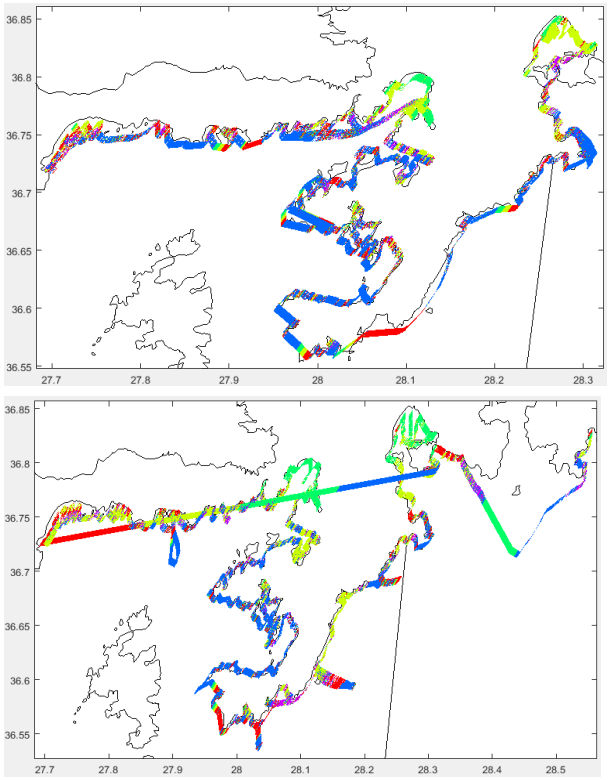

Figure 9. Bottom types in winter (left panel) and summer (right panel) from east to west direction of the study area.

To enhance habitat characterization, the percent coverage of submerged plants on the seabed was evaluated. Approximately 100% coverage indicated the presence of *P. oceanica*, which was in good agreement with POSIBIOM results across the study area (Figures 4, S6). Outside the seagrass beds, coverage was generally less than 30%, and predominantly below 10%. Mutlu et al. (62 2022c) reported that *Caulerpa prolifera* and *C. taxifolia* var. *distincophylla* dominated the Antalya Gulf, whereas coastal waters of the Finike and Kekova bays were mainly dominated by *Cymodocea nodosa* [60]. In contrast, the Taşucu Gulf exhibited a distinct pattern of bottom types and plant coverage, ranging between more than 20% and less than 90% (Figures 9, S6). With respect to plant or canopy height estimated by Visual Aquatic, *P. oceanica* beds exhibited canopy heights of less than 35 cm in winter, while values ranged between 35 and 70 cm in summer. In other regions, plant length was generally less than 20 cm (Figure S7).

Sediment Thickness

Sediment thickness estimates are shown in Figure S8. Thickness varied between 0.8 and 0.9 m, as the 206 kHz acoustic signal penetrated the seabed and measurements were derived from the length of the first echo tail. Between Anamur and Taşucu, sediment thickness was greater in summer than in winter, with a difference of approximately 3–4 cm. In the Antalya Gulf, coastal and rocky bottoms exhibited sediment thicknesses of less than 0.85 m, followed by thicker sediments at greater depths. West of Antalya, sediment thickness increased progressively toward the west. No seasonal or regional differences in sediment thickness were observed on seagrass beds, where values remained around 0.85–0.90 m in both eastern and western regions (Figure S8).

3.2.4. Ecological Evaluation

The present study aimed to evaluate relationships between estimated and measured biometrics, environmental variables, and ecological status. Ecological status was assessed using criteria based on threshold limits and ranges of shoot density at each bottom depth, following UNEP/MAP-RAC/SPA [7, 11].

 doi:10.20944/preprints202603.1020.v1

Ecology

Non-metric multidimensional scaling (nMDS) revealed similar configurations between acoustic and SCUBA-based datasets (Figure 10a, b), with a significant correlation confirmed by RELATE analysis ($r = 0.132$, $p = 0.03$). For both methods, biometrics differed significantly by season and bottom type (Table 5). Interactions between season and bottom type influenced biometrics only in the acoustic estimates. When data from acoustic and SCUBA methods were pooled, no significant differences in biometrics were detected between methods (Table 5, Figure 10c). Excluding depth, interactions between method and other factors significantly influenced biometric variability. Consistent with the separate method analyses, the interaction between season and bottom type significantly affected biometric variation ($p < 0.05$; Table 5). A clear seasonal separation was also evident in the pooled dataset (Table 5, Figure 10d).

Table 5. Three- and four-way PerMANOVA test or a difference in the biometrics of *Posidonia oceanica* estimated by acoustical (Ac) and SCUBA (Sc) samplings among seasons, bottom depths and types, and included method with their interactions, respectively. Bold p value denotes significant difference at $p < 0.05$. Permutation number was 999.

	Acoustic			**SCUBA**			**Ac & Sc**		
Source	**df**	**p**	**p(MC)**	**df**	**p**	**p(MC)**	**df**	**p**	**p(MC)**
Method							1	0.333	0.309
Season	1	**0.001**	**0.001**	1	**0.001**	**0.001**	1	**0.001**	**0.001**
Type	3	**0.006**	**0.005**	3	**0.022**	**0.004**	3	0.184	0.182
Depth	6	0.738	0.785	5	0.053	**0.017**	6	0.368	0.383
Method x Season							1	**0.003**	**0.002**
Method x Type							3	**0.002**	**0.001**
Method x Depth							5	0.079	0.055
Season x Type	3	**0.017**	**0.01**	3	0.735	0.782	3	**0.036**	**0.026**
Season x Depth	3	0.248	0.233	3	0.767	0.788	3	0.304	0.34
Type x Depth	14	0.976	0.972	15	0.99	0.996	15	0.989	0.994
Method x Season x Type							3	0.16	0.148
Method x Season x Depth							3	0.556	0.521
Method x Type x Depth							14	0.982	0.993
Season x Type x Depth	6	0.887	0.911	6	0.766	0.794	6	0.898	0.926
Method x Season x Type x Depth							6	0.816	0.819
Residuals	104			110			214		
Total	140			146			287		

Unlike the number of leaves per shoot (Lno) and leaf length (L), shoot density (S) was higher in winter for both methods (Figure 10a, c). Explanatory environmental factors for leaf biomass and leaf area index were not resolved in the nMDS ordination (Figure 10a, b). For the pooled dataset, Lno and L were higher in summer than in winter (Figure 10c, d), consistent with patterns observed in the unpooled acoustic and SCUBA datasets (Figure 10a, b).

 doi:10.20944/preprints202603.1020.v1

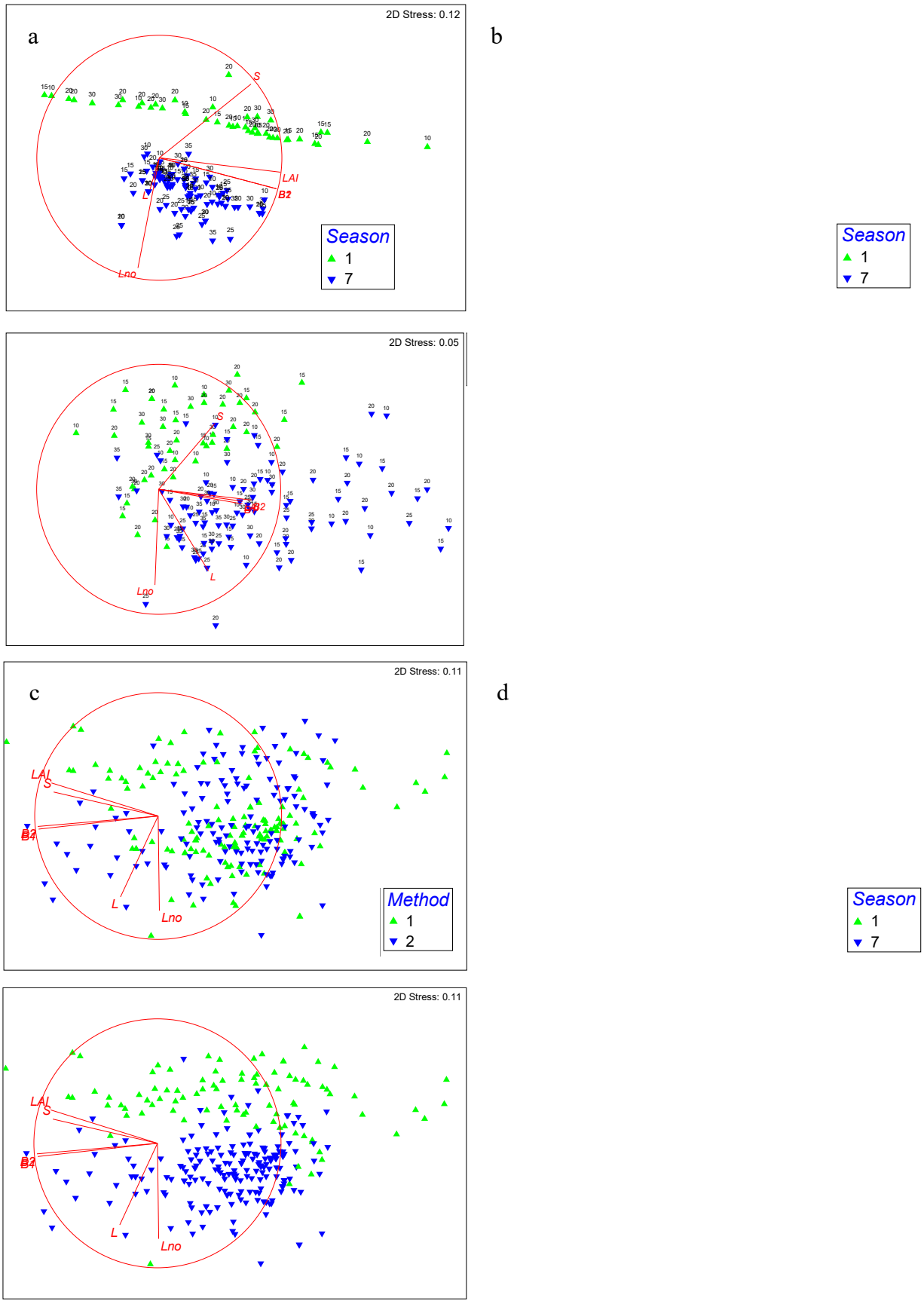

Figure 10. nMDS plot of the biometrics from acoustical (a) and SCUBA sampling stations (b) classified by seasons in symbol, and by bottom depths in labels and pooled data of methods (1: Acoustics, and 2: SCUBA) for the stations classified by methods (c) and seasons (1: winter and 7: summer) (d).

 doi:10.20944/preprints202603.1020.v1

Canonical correspondence analysis (CCA) plots were resolved and configured separately for winter and summer, for acoustic and SCUBA datasets, and for the combined dataset, using both common and season-specific environmental parameters (Figures 11, S9–S11), with corresponding results summarized in Tables S2–S4. Individual CCA analyses for each season and method are presented in Table S2 and Figure S9. In winter, the primary explanatory variables were temperature in the two water layers (sea surface and near-bottom), which were strongly correlated with CCA1 for both methods, followed by Secchi disk depth (Table S2, Figure S9). Dissolved oxygen in both layers was negatively correlated with Lno and L, followed by S in the acoustic dataset, whereas in the SCUBA dataset it was negatively correlated with LAI and S, highlighting methodological contrasts, particularly in relation to Secchi disk depth. CCA1 explained 95.0% and 99.9% of the variance in the acoustic and SCUBA datasets, respectively, and these relationships were validated by Monte Carlo permutation tests ($F = 37.21$, $p = 0.001$ for acoustics; $F = 12.44$, $p = 0.002$ for SCUBA). In summer, CCA1 explained 76.7% and 88.2% of the variance in the biometrics–environment relationships for the acoustic and SCUBA datasets, respectively (Table S2, Figure S9). For both methods, Secchi disk depth was the primary variable driving discrimination along CCA1, followed by near-bottom temperature, with contrasting associations between biometrics and environmental variables across methods. The robustness of these relationships was confirmed by Monte Carlo tests ($F = 8.99$, $p = 0.000$ for acoustics; $F = 25.90$, $p = 0.002$ for SCUBA). No significant discrimination or explanatory variables were identified along CCA2 for any of the individual seasonal or methodological configurations (Table S2). Bottom depth did not exert a significant influence on biometrics in either season or method (Figure S9), whereas bottom type showed a clear structuring effect (Figure S10).

When common environmental parameters were used for both seasons, including physical variables from the two water layers and Secchi disk depth, clear seasonal separation was observed for both methods (Table S3, Figure 11). Seasonal discrimination along CCA1 was driven primarily by negative correlations with temperature in both layers, contrasted with positive correlations with near-bottom salinity. In both methods, shoot density (S) was positively correlated with CCA1. In contrast, Lno and L were negatively correlated with CCA1 in the acoustic dataset, whereas LAI and L showed negative correlations in the SCUBA dataset (Figure 11). Overall, CCA1 reflected opposing influences of near-bottom salinity and water temperature on seagrass biometrics. Along CCA2, L and LAI were positively and negatively correlated, respectively, and both were associated with Secchi disk depth in both methods. Additionally, CCA2 was negatively correlated with sea-surface pH in the acoustic dataset and with near-bottom salinity in the SCUBA dataset (Table S3, Figure 11). These relationships were statistically supported by Monte Carlo permutation tests ($F = 112.8$, $p = 0.002$ for acoustics; $F = 48.11$, $p = 0.002$ for SCUBA).

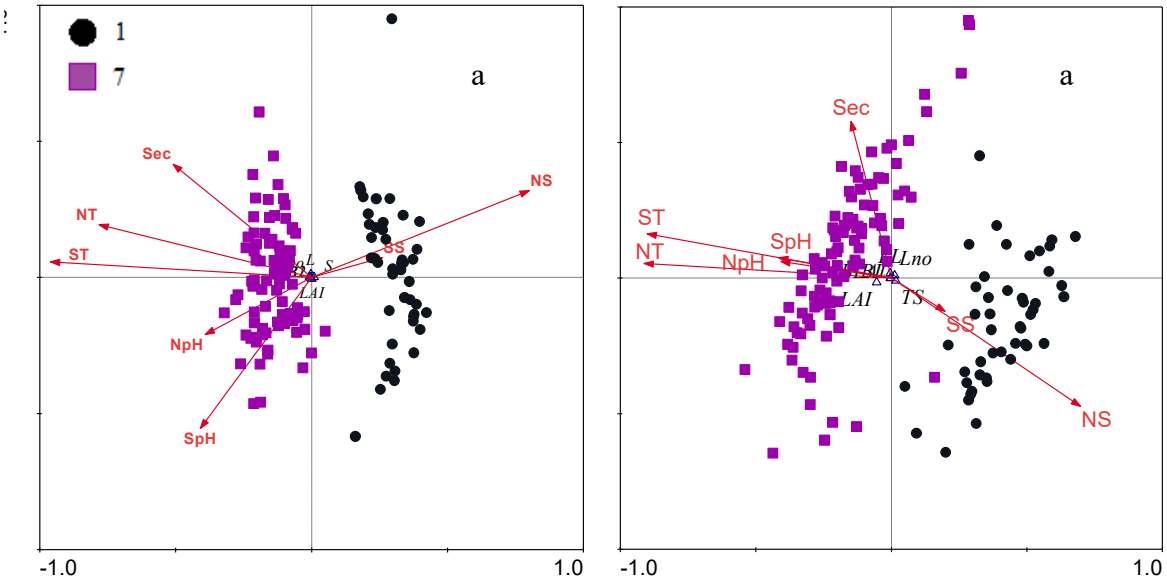

 doi:10.20944/preprints202603.1020.v1

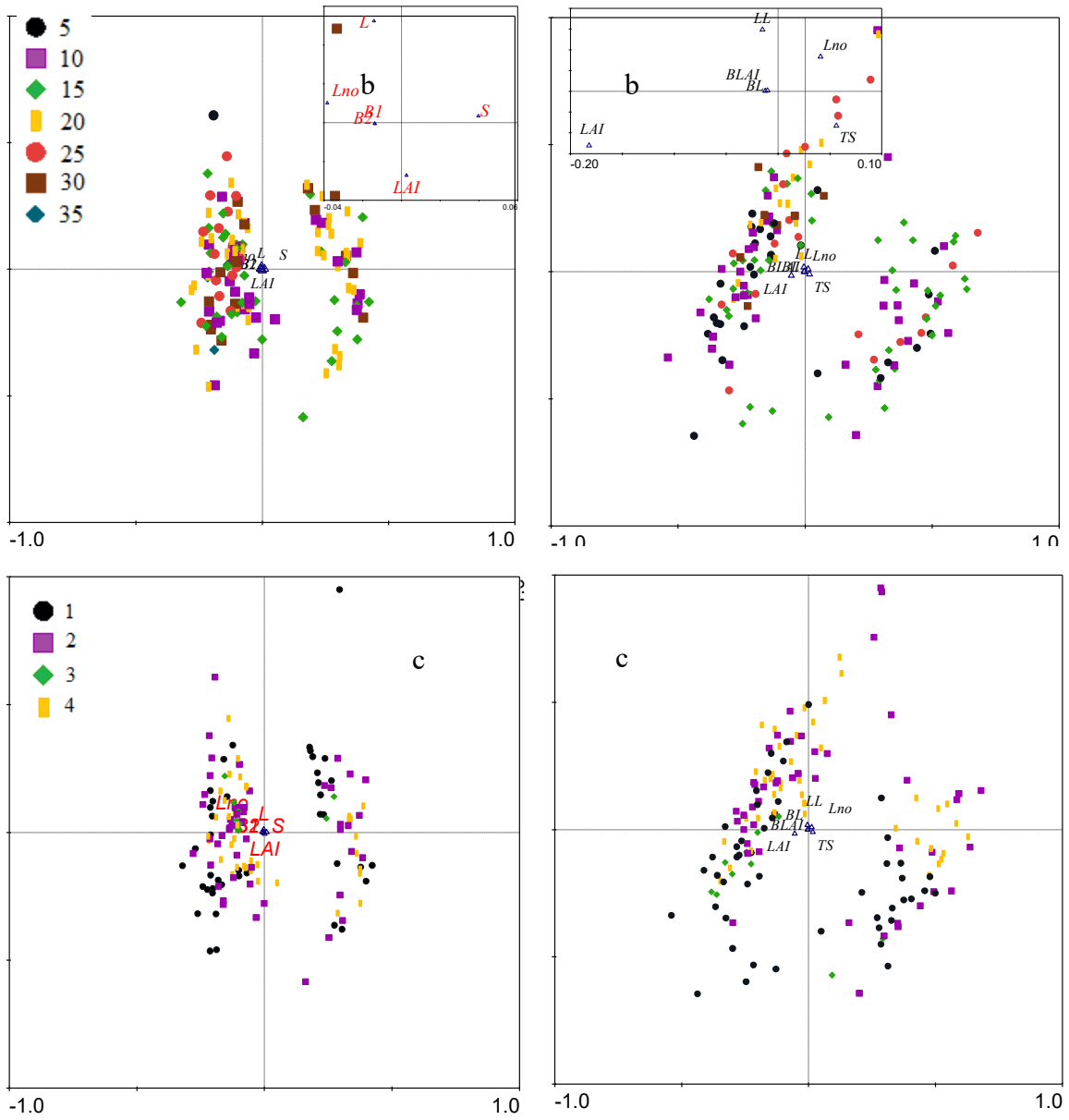

Figure 11. Triplot of CCA for the biometrics estimated from acoustical (left panel) and SCUBA (right panel) sampling stations classified by seasons; 1: winter and 7: summer (a), bottom depths with biometric scattering zoom-in plot (b) and bottom types; 1: rock, 2: sand, 3: matte and 4: mud (c). For the biometrics, BL: B1, BLAI: B2, LL: L and TS: S for SCUBA sampling (see Table S4 for the environmental variable description).

Only in summer, when physical and chemical parameters were measured in both water layers, were common variables correlated with CCA1 for both acoustic and SCUBA methods. These variables were Secchi disk depth (positive correlation), near-bottom temperature (negative correlation), and nitrate (NO_3^-; positive correlation) (Table S4, Figure S11). Among the common biometrics, leaf length was positively correlated with CCA1, whereas L and LAI were negatively correlated with CCA2. CCA2 was positively correlated with nitrogen-based nutrients in the acoustic dataset, while in the SCUBA dataset it was associated only with sea-surface temperature and phosphate (PO_4^{3-}) (Table S4, Figure S11). CCA1 explained more than half of the total variance in the biometrics–environment relationships, accounting for 65.6% in the acoustic dataset and 87.6% in the SCUBA dataset. The discrimination along CCA1 was validated by Monte Carlo permutation tests for both methods ($F = 17.95$, $p = 0.038$ for acoustics; $F = 35.78$, $p = 0.006$ for SCUBA). Across all CCA configurations presented here, Spearman rank correlations between biometrics and environmental

 doi:10.20944/preprints202603.1020.v1

variables were consistently high and statistically significant along the CCA1 axis for both methods (Tables S2–S4).

Ecological Status

For *Posidonia oceanica*, the ecological status of each location was determined using shoot density criteria applied to all seasons, based on depth-specific density thresholds for each bottom depth [11] and specifically at 15 m depth following UNEP/MAP-RAC/SPA [7]. The present study further evaluated the concordance in ecological status classification between acoustic and SCUBA-based assessments (Figure 12).

Overall, ecological status was classified as good to high east of the Antalya city centre, whereas it ranged from poor to moderate–good west of Antalya in both seasons and for both methods. However, the Side meadows were classified as moderate in both winter and summer based on SCUBA observations (Figure 12). In general, ecological status was higher in summer than in winter. Acoustic assessments tended to overestimate ecological status by approximately one class relative to SCUBA-based estimates (Figure 12). Nevertheless, between Kekova and the westernmost sampling locations (excluding Datça Bay), areas characterized by intense touristic activity during summer [13], ecological status was higher in winter than in summer (Figure 12). Despite these differences, there was overall good concordance between acoustic and SCUBA methods in the classification of ecological status.

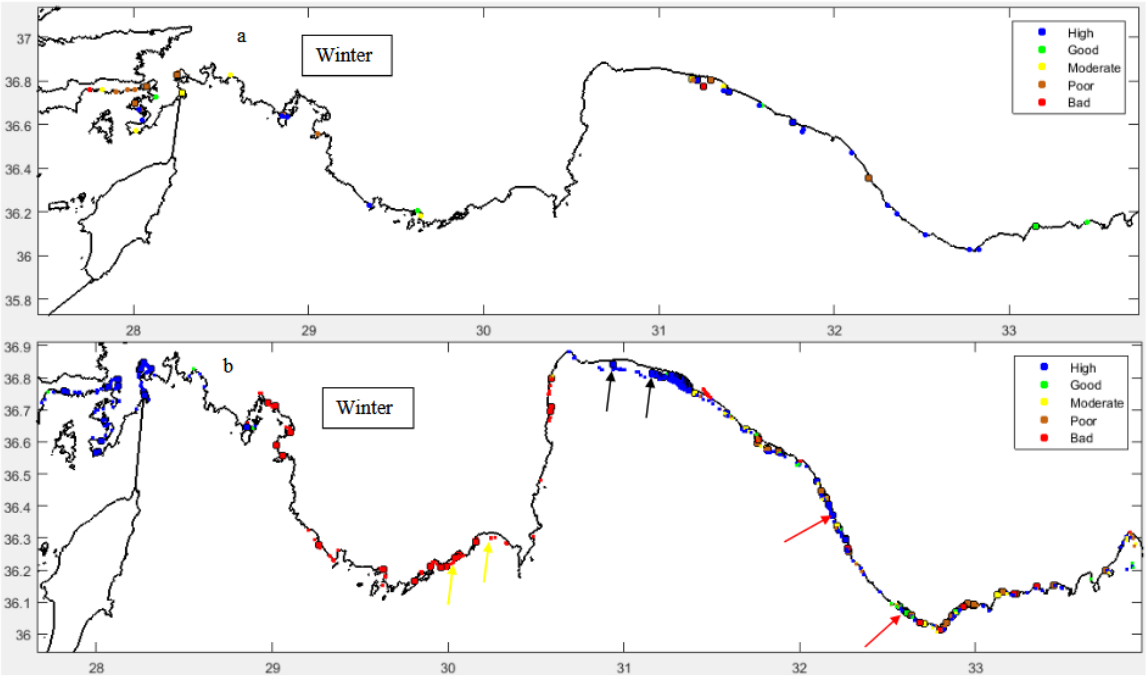

 doi:10.20944/preprints202603.1020.v1

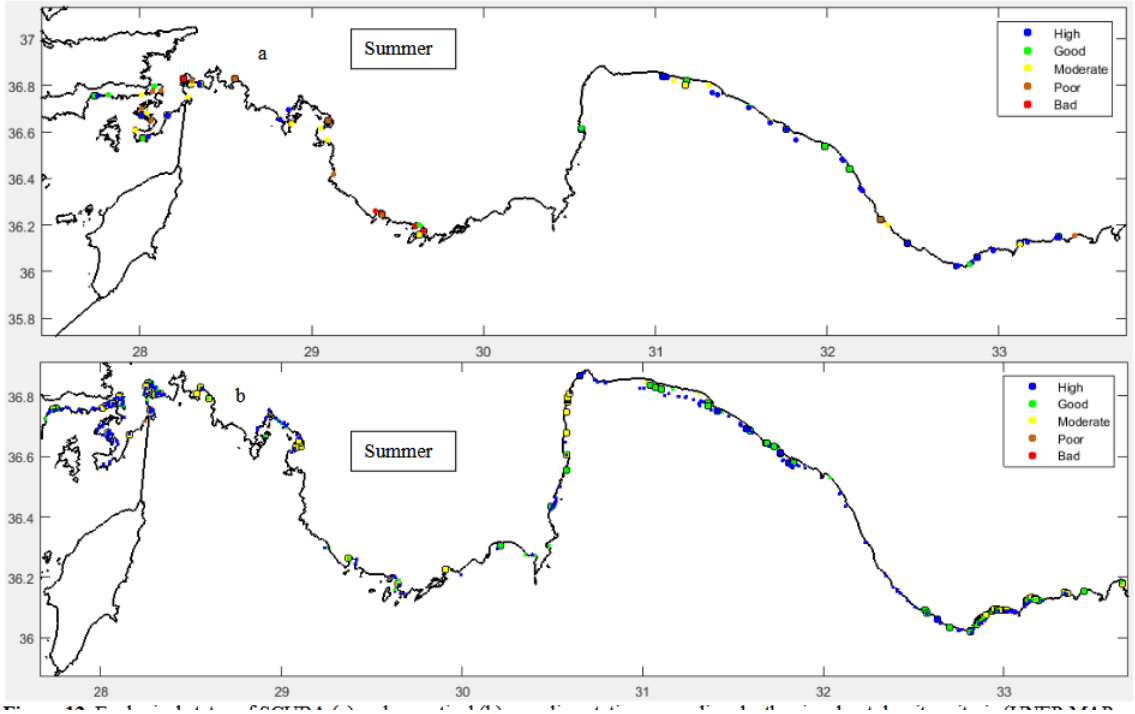

Figure 12. Ecological status of SCUBA (a) and acoustical (b) sampling stations regarding depth-wise shoot density criteria (UNEP-MAP-RAC/SPA, 2015) in winter and summer. The larger marker showed the status according to a criterion specified at 15 m [7]. Black arrow denotes *Caulerpa prolifera*, yellow *Cymodocea nodosa* and red a biased detection of *P. oceanica* due to the significantly tilted transducer.

4. Discussion

4.1. Agreement and Bias Between Acoustic and SCUBA-Based Biometrics

Overall, the acoustic estimates tended to overestimate all biometrics relative to the SCUBA measurements (Figure A2a). The regression model was significant ($p < 0.05$) for all biometrics (Table A1; Figure A2). However, when the measured variable was evaluated alongside other model terms, it was not significant at the 5% level for half of the biometrics (L, S, and Lno; Table A2). Measured values, bottom depth, and bottom type did not significantly influence the acoustic estimates, whereas season exerted a significant effect on S and Lno ($p < 0.05$), with the exception of leaf length (L). The model explained more than 72% of the variability in the significant response variables (S and Lno) with respect to predictive variables during summer (Table A1; Figure A2). Using a robust fitting approach, depth differentiated estimates of L, and season produced significant changes in S and Lno (Table A2); however, the model was significantly fitted only for S and Lno.

Regression equations linking measured biomass (SCUBA) to other density-related variables (LAI and S) of *Posidonia oceanica* were previously established to convert acoustically estimated leaf biomass into estimated LAI and S along the entire Turkish Mediterranean coast [14]. Accordingly, leaf biomass and leaf length estimated using the software package POSIBiom [49] can be used to derive LAI and S without the need for SCUBA sampling in protected meadows, although ground-truth sampling is still strongly recommended. SCUBA sampling in these vulnerable meadows is undesirable due to its destructive effects on both below- and above-ground biomass. Owing to its invasive nature, SCUBA sampling typically limits the number of shoots that can be collected (13,29-30].

Season-specific acoustic–biomass conversion equations have previously been established; however, these were based on samples collected at a single depth (15 m) [50]. A depth of 15 m represents a critical threshold for classifying shallow versus deep seagrass meadows and induces marked differences in plant traits. Consequently, biometric variance at this depth is high, resulting

 doi:10.20944/preprints202603.1020.v1

in unstable biometric distributions. Additional high variance was observed in biometrics measured in August, followed by structural differences associated with bottom type within the study area [14]. In contrast, Mutlu et al. [58] demonstrated that acoustic estimates underestimated biometrics relative to SCUBA measurements in a limited part of the present study area, highlighting regional variability. Therefore, perfect agreement between acoustic estimates and direct measurements should not be expected. Differences between methods likely arise from depth-dependent variations in acoustic scattering properties, as discussed by Mutlu and Olguner [50], including seasonal changes in lime structures within seagrass tissues [63], porosity and gas inclusion during calcite formation on leaves [64], and peak calcification and photosynthetic activity between May and August [65]. To reduce these uncertainties, an ongoing project is investigating the acoustic scattering properties of adult, young, and juvenile leaves collected across different seasons, depths, regions, and bottom types [61]. The outcomes of this project will support future upgrades of POSIBiom through the integration of regression models that explicitly account for bottom depth and bottom type, thereby improving estimation accuracy. Among the biometrics, leaf length represents a true linear measurement in SCUBA samples, whereas acoustically it corresponds to canopy height, which varies depending on leaf orientation; this introduces an inherent methodological difference between the two approaches [58].

Lno and acoustically estimated biomass exhibited a complete nugget-effect dispersal pattern, characterized by a zero slope. This pattern raises questions regarding the suitability of using this relationship for biometric conversion from biomass. Indeed, the O-shaped distribution of data points observed between variables indicates inconsistent estimates and a correlation coefficient of zero, suggesting that such relationships should not be used. Another limitation is the inability to directly estimate Lno, as two variables were averaged in contrast to individual measurement–estimate comparisons. This limitation also applies to other biometric estimates, with the exception of L. Leaf length (L) is measured directly from SCUBA samples regardless of leaf orientation (upright, semi-upright, or flat), whereas acoustically L is estimated based on leaf orientation and is referred to as canopy height in remote sensing applications.

4.2. Spatiotemporal Distribution

4.2.1. Biometrics

Temporal variation in *P. oceanica* is more pronounced for leaf biomass, LAI, and leaf length (L) than for shoot density (S), as older leaves are typically shed during August–September [66]. Mutlu [49] emphasized temporal detection limits of vertical rhizome growth using echosounder data processed with POSIBiom [12-13]. Acoustic differentiation between the dominant seagrass species *P. oceanica* and *Cymodocea nodosa* along the Turkish Mediterranean coast has also been demonstrated [50-51].

The spatiotemporal distribution of *P. oceanica* is governed by hydrography, atmospheric forcing, and substrate characteristics, with substrate being particularly critical for recolonization through vegetative fragments [17,21, 67-68]. Meadow depth limits vary with substrate type, ranging from 0.5–1 m to 33–43 m in the western Mediterranean [15, 69], with similar limits reported for the eastern Mediterranean [14]. Water velocity influences meadow expansion and structure [70-71]. Sediment calcium carbonate content is a key factor: high percentages in the Antalya Gulf (70–90%) support extensive meadows, whereas low contents in the Finike Gulf and Kekova Bay (10–30%) correspond to the absence of meadows, and intermediate values in Kaş Bay (45–60%) support smaller beds [13-14,72]. Calcium carbonate and carbon are essential components in leaf and rhizome development [73-74].

Environmental variables exert strong control over biometric traits. Shoot density (S) varies with location, depth, wind exposure, substrate type, and seabed slope [18, 75]. Intermediate depths (~15 m) show particularly high variability, likely due to reduced photosynthetically active radiation (PAR) [12,14, 76]. Leaf biomass, which has been comparatively understudied, reflects seasonal meadow

 doi:10.20944/preprints202603.1020.v1

condition, following an annual growth cycle in healthy meadows but becoming disrupted in degraded systems [77-80]. In contrast, S and LAI exhibit limited temporal variability in healthy meadows [80-82]. Substrate type strongly influences biometrics. Meadow coverage exceeds 75% on rocky substrates but declines to 50–75% on sand or fine sand [83]. LAI decreases with depth and is approximately 42% lower on rock than on sand or matte substrates [84-85]. Leaf area is reduced on rocky bottoms, likely reflecting differences in anchorage conditions and nutrient availability [86-87]. Shoot density may double on hard substrates compared with soft substrates and is highest on rocky bottoms [15-16, 19]. This pattern inversely correlates with leaf area, reflecting phenotypic plasticity [88-89]. Seasonal variability is greatest on rocky and sandy substrates during winter and on rigid substrates during summer [75].

Leaf length (L) exhibits less consistent patterns with respect to substrate and depth. It generally decreases with depth, increasing from winter (15 °C) to spring (21 °C) at salinities below 39 PSU, declining slightly by July (27 °C, 39 PSU), and decreasing further during August–September (28–29 °C, ~40 PSU) in the Antalya Gulf [12]. Elevated salinity-induced mortality has been documented [90]. Leaf length growth depends on leaf type, substrate, depth, seasonal temperature, and herbivory pressure [77-78, 80-81,85, 91-92]. Maximum leaf length occurs at approximately 10 m depth in June–July and at 30 m depth with a two-month delay, likely due to reduced hydrodynamic stress at greater depths [81,91-92].

4.2.2. Habitats

Recent EU initiatives emphasize the assessment of *Posidonia oceanica* meadow habitats along the Turkish and broader Mediterranean coasts [93], supporting projects under upcoming funding calls. In this context, habitats were classified based on two primary characteristics—bottom type and sediment thickness—both of which can be estimated using acoustic data. Moreover, in a particular part of the study area with largest meadow beds [12,58,94], the Antalya Gulf, habitat degradation has recently accelerated due to touristic activities aimed at recreational use. These activities include sand pumping from greater depths into very shallow waters and the mechanical breaking of rocky substrata to artificially create sandy bottoms. In addition to global warming, natural and anthropogenic effluents and impacts, such human-induced disturbances have damaged the seagrass meadow by partially covering the habitat and vegetation with sand and by causing the loss of rocky substrata together with their associated vegetation. This degradation is evident from comparisons of acoustically derived bottom types obtained from surveys conducted in 2011–2012, 2014–2015, 2019, and 2024–2025 [12, 58-59, 61, 94-95; personal communications in 2025-2026). In 2025 May survey, half lengths of leaves of *P. oceanica* on rocks were observed to be buried in artificially sand accumulated-layered [59], which were never observed in the previous studies in 1.5 decades [12, 58-59, 61, 94-95].

Bottom Types

Of habitat categories defined by the EU Habitats Directive (92/43/EEC) five were identified during the present study. This classification encompasses most of the habitat types considered here as bottom types [13]. During calibration of the acoustic data, the system did not discriminate between rocky bottoms, seagrass meadows, and matte structures; these were therefore classified collectively as hard substrata, which coincided well with meadow distribution [14]. This outcome likely reflects similar acoustic reflection coefficients among these materials. Improved discrimination may be achieved through finer calibration or the use of multiple frequencies, as different frequencies respond differently to material properties of targets [48, 96]. In the present study, a single frequency was employed. Frequency-response analysis is commonly used for detailed acoustic target characterization, such as fish species identification or discrimination among abiotic (thermocline, halocline) and biotic (zooplankton) scatterers within mixed layers, based on frequency-dependent responses to material properties and target size [97]. Sound penetration into sediments is limited by frequency, system configuration, and source level [97]. Using this approach, slimy and rough fractions of sand and mud were distinguished alongside hard substrata.

 doi:10.20944/preprints202603.1020.v1

Bottom type and substrate are critical determinants of *P. oceanica* biometric responses, which differ markedly between soft and hard substrates [15-16, 18]. Substrate type influences dispersal patterns, spatial distribution, and depth boundaries of *P. oceanica* meadows [15-17], reflecting species-specific responses of seedlings and root hairs during early development to physical substrate characteristics [21]. Together with hydrodynamic forces [70], these responses determine substrate suitability for meadow establishment and persistence. Human activities may also affect the upper depth limit of meadows [71]. Consequently, bottom type generates variation in several biometrics [19, 21, 75, 83, 85]. Collectively, this factor influences biometrics, which remains a critical metric for ecological status assessment of seagrass meadows as updated by Dalmau et al. [93] referring Mutlu et al. [14].

Sediment thickness

Assessment of sediment thickness and bottom type is valuable for monitoring seabed changes associated with human activities, such as sand extraction, coastal nourishment, dredging, and harbor deepening. Finer sediments tend to accumulate in thicker layers, whereas coarse and hard materials are associated with thinner sediment cover. Bottom hardness and roughness can be quantified acoustically; however, estimation may be biased when the transducer is tilted relative to the seabed, as observed in parts of the study area during winter surveys. Soft, fine sediments exhibited thicker textures than hard, coarse materials, resulting in minimal sediment cover on rocky and rough sandy substrates. Mutlu et al. [59] conducted a seasonal acoustic study in the Side meadow beds, a subset of the present study area, demonstrating that flat rock surfaces (10–30 cm relief) were seasonally covered by sand, with sediment thickness increasing notably in May 2025 relative to other seasons (September 2024; January and July 2025). These findings were independently confirmed by SCUBA divers.

4.2.3. Ecological Evaluation

Ecology

Interannual dynamics of *P. oceanica* are primarily controlled by nutrient availability, carbon supply, and light conditions [84, 98]. Spatial variables—particularly bottom depth—followed by season and water temperature, strongly shape biometric–environment relationships for both measured and acoustically estimated data, as revealed by redundancy analysis (RDA). Depth is the dominant driver of population structure and biometric variability, with season exerting a secondary influence, resulting in distinct seasonal patterns across shallow (5–10 m), transition (~15 m), and deep (20–30 m) zones. Samples from the transition zone cluster around the center of the RDA ordination, reflecting elevated seasonal variability. The 15 m depth zone is particularly distinctive, exhibiting reduced photosynthetic activity compared with 5 m and 30 m depths, likely due to solar irradiance effects [99]. Generalized additive models (GAMs) indicated that, excluding depth, salinity negatively influences density-related metrics, whereas water density and Secchi depth have positive effects; near-bottom oxygen concentration positively affects below-ground components.

Leaf length (LL) is more sensitive to environmental variables than density metrics. Negative drivers include temperature, sediment $CaCO_3$ content, silt, phosphate, and PAR, whereas Secchi depth, nitrogen-based nutrients (excluding ammonium), and pH exert positive effects. Additional shading from leaves and epiphytes further reduces light availability, particularly between May and August/October [91, 100]. *P. oceanica* utilizes $CaCO_3$ and carbon in leaf and rhizome development [73-74]. Nitrogen affects biometrics differentially, reducing leaf width while increasing leaf number per shoot. Seasonal nutrient limitation, especially from late spring through autumn, constrains growth [98].

Nodal (inter-shoot) distance is influenced by optical and physicochemical parameters, notably temperature, salinity, phosphate, and nitrite+nitrate concentrations [12]. Nitrogen uptake occurs primarily via roots during winter and early spring, when water-column concentrations are highest.

 doi:10.20944/preprints202603.1020.v1

Generalized linear models (GLMs) revealed linear relationships between leaf biomass, shoot density, and environmental parameters, but not for LAI or LL, suggesting partially linear responses with threshold behavior. RDA corroborated these findings, with $CaCO_3$ consistently exerting positive effects on biometrics, more pronounced in measured than in acoustically estimated data. Leaf calcification peaks between May and August, coinciding with maximum photosynthetic activity [65, 101], and elevated $CaCO_3$ enhances acoustic scattering through density and sound-velocity contrasts [63, 102].

Other biometrics are regulated by specific physical and chemical drivers: leaf number by nitrogen availability, inter-shoot distance by optical properties, leaf width by sediment total organic carbon (which negatively affects rhizome traits), LL by pH and nitrogen, vertical rhizome length by temperature and density, and shoot density by water density [12].

Ecological Status

Based on shoot density within each classified depth zone, estimated and measured assessments of ecological status showed strong concordance. Biometrics, including shoot density, differed significantly among bottom types [19, 21, 75, 83, 85]. Density-related variables were higher on hard substrates than on soft substrates, whereas inter-nodal distance was greater on matte than on rock, sand, or mud, in contrast to leaf biomass patterns [15-16, 18]. Mud exhibited the lowest leaf number per shoot and shoot density, whereas rocky substrates showed the highest values. The shortest rhizomes were observed on rock, while the longest occurred on matte, which also supported the longest leaves. Soft substrates exhibited wider leaves than hard substrates. In addition to seasonal and depth-related variability, biometrics clustered distinctly between rock and mud habitats. In contrast to morphometric traits, density metrics decreased linearly from hard to soft substrates [14].

Water-column nutrients, particularly surface-water ammonium and phosphate, reduced ecological status [12], with maximum nutrient concentrations corresponding to poor and bad status classifications during summer, consistent with observations by Karaca et al. [103]. Although ammonium is utilized by aquatic flora [104], excess concentrations can be toxic, potentially reducing shoot density through seagrass mortality. Additionally, elevated temperature and salinity disrupt osmotic regulation in seagrass leaves, leading to cell rupture and mass leaf mortality in late summer [90, 105]. Despite these stressors, no spatial differences in ecological status were detected between winter and summer, likely reflecting the influence of ongoing global warming; for example, temperatures of up to 32 °C have been recorded during the past decade along the Turkish Mediterranean coast. One consequence of global warming is increased flowering of *P. oceanica* as a mode of sexual reproduction instead of clonal expansion; however, in the present study area, only two flowering events have been observed over the past 1.5 decades, likely due to nitrogen limitation in the oligotrophic Levantine Sea [10, 19]. Collectively, these factors influence shoot density, which remains a critical metric for ecological status assessment of seagrass meadows [93].

5. Conclusions

As a conservation-oriented approach for protected seagrass meadows, non-destructive remote sensing techniques, particularly acoustic methods, represent an effective tool for estimating seagrass biometrics. Acoustic monitoring of seagrasses was initiated through a dedicated project in 2011 [94]. Subsequent studies demonstrated that *Posidonia oceanica* and *Cymodocea nodosa* exhibit distinct acoustic responses at 200 kHz, and that *P. oceanica* displays clear seasonal variability in its acoustic scattering structure [50-51]. However, these earlier investigations were restricted to structural estimates derived from specimens collected at 15 m depth, which formed the basis for the seasonal conversion equations applied in the present study. Depth-related variability in acoustic responses had not been addressed until the ongoing project by Mutlu et al. [59], which explicitly incorporates depth-dependent effects and leaf-type differences. Accounting for such depth-wise variability in plant acoustic reflectance is a critical step toward improving the accuracy of biometric estimations. As relationships among infra-biometrics are further refined and detailed acoustic structures are

 doi:10.20944/preprints202603.1020.v1

resolved—particularly through the use of multi-frequency systems—future studies will enable more accurate and precise biometric assessments and, consequently, ecological status evaluations with high confidence and minimal reliance on sea-truthing. The advancement of these methodologies will facilitate rapid, large-scale assessments of seagrass biometrics, habitats (Figure S12), ecological conditions (when supported by environmental measurements), and ecosystem status across gradients ranging from degraded to pristine. Such developments are particularly timely as current ecological assessment criteria [7, 11] continue to be updated through international collaboration and the integration of recent scientific findings (e.g. [93]).

Supplementary Materials: Table S1. Equations established to convert leaf biomass based on leaf area (B2 in g/m^2, Equation 1) and leaf length (B1 in g/m^2, Equation 2) to single-sided leaf area (LA in cm^2/m^2), shoot density (S in shoots/m^2) and number of leaf number per shoot (Lno ind/S) using the measured data. Pearson correlation coefficients (r_1 and r_2 for equations 1 and 2, respectively, and bold values denote significantly correlated at $p < 0.05$) and sample size (n) based on the number of sampling stations (modified from Mutlu et al., 2026). **Figure S1.** Pos-hoc test (LDS, Tukey) of the biometrics estimated from acoustic (left panel) and SCUBA (right panel) sampling by bottom depths in winter (blue mark; to be tested among the depths, red: significantly different, grey: significantly not different between vertical discrete grey lines). **Figure S2.** Pos-hoc test (LDS, Tukey) of the biometrics estimated from acoustic (left panel) and SCUBA (right panel) sampling by bottom types in winter (blue mark; to be tested among the types, red: significantly different, grey: significantly not different between vertical discrete grey lines). **Figure S3.** Pos-hoc test (LDS, Tukey) of the biometrics estimated from acoustic (left panel) and SCUBA (right panel) sampling by bottom depths in summer (blue mark; to be tested among the depths, red: significantly different, grey: significantly not different between vertical discrete grey lines). **Figure S4**. Pos-hoc test (LDS, Tukey) of the biometrics estimated from acoustic (left panel) and SCUBA (right panel) sampling by bottom types in summer (blue mark; to be tested among the types, red: significantly different, grey: significantly not different between vertical discrete grey lines). **Figure S5** . Pos-hoc test (LDS, Tukey) of the biometrics estimated from acoustic (left panel) and SCUBA (right panel) sampling by season (blue mark; to be tested among the seasons, red: significantly different, grey: significantly not different between vertical discrete grey lines). **Figure S6.** Percent coverage area by submerged plants in winter (left panel) and summer (right panel). Red arrow denotes misinterpreted area in winter. **Figure S7.** Canopy height (m) of submerged plants in winter (left panel) and summer (right panel). Red arrow denotes misinterpreted area in winter. **Figure S8.** Sediment thickness (m) estimated by VBT in winter (left panel) and summer (right panel) from east to west of the study area. **Table S2.** Summary of statistical measures of physical environmental parameters of CCA correlation configured in Figures 10 (prefix of variables; SS: sea surface and N: Near-bottom water) with the biometrics for each season and method (see Table S4 for the variable description). **Figure S9**. Triplot of CCA for the biometrics estimated from acoustical (upper panel) and SCUBA (lower panel) sampling stations classified by bottom depths in winter (left panel) and summer (right panel) including physical environmental parameters. For the biometrics of SCUBA, BL: B1, BLAI: B2, LL: L and TS: S (see Table S4 for the variable description). **Figure S10.** Triplot of CCA overlapped CCA in Figure S7 for the biometrics estimated from acoustical (upper panel) and SCUBA (lower panel) sampling stations classified by bottom types; 1: rock, 2: sand, 3: *matte* and 4: mud (c) depths in winter (left panel) and summer (right panel) (see Fig S9 for detailed CCA configuration) including physical environmental parameters. For the biometrics of SCUBA, BL: B1, BLAI: B2, LL: L and TS: S. (see Table S4 for the variable description). **Table S3**. Summary of statistical measures of physical environmental parameters of CCA correlation configured in Figure S9-S10 (prefix of variables; SS: sea surface and N: Near-bottom water) with the biometrics for combined season and each method (see Table S4 for the variable description). **Table S4.** Summary of statistical measures of all environmental parameters of CCA correlation configured in Figure S10 (prefix of variables; SS: sea surface and N: Near-bottom water) with the biometrics in summer for each method**. Figure S11**. Triplot of CCA for the biometrics estimated from acoustical (left panel) and SCUBA (right panel) sampling stations classified by bottom depths (upper panel) and bottom types; 1: rock, 2: sand, 3: *matte* and 4: mud (lower panel) in summer including all environmental parameters. For the biometrics, BL: B1, BLAI: B2, LL: L and TS: S (see Table S4 for the variable description). **Figure S12.** Bottom types unclassified in winter (left panel) and summer (right panel).

 doi:10.20944/preprints202603.1020.v1

Funding: This research was funded by the Scientific and Technical Research Council of Turkey, TUBITAK. Grant no: 117Y133.

Data Availability Statement: The raw data supporting the conclusions of this article will be made available by the author on request.

Acknowledgments: This study was funded by The Scientific and Technical Research Council of Turkey (TUBITAK) with grant no: 117Y133. I thank project team (Yaşar Özvarol and Ahmet Şahin) and crews of R/V "Akdeniz Su" for their helps onboard.

Conflicts of Interest: The authors declare no conflicts of interest.

References

1. Strydom, S.; Murray, K.; Moustaka, M.; Hyndes, G.; Wilson, S. Getting edgy: implications of fragmented seagrass meadows for fish assemblages. *Landsc. Ecol.* 2026, *41*, 31. https://doi.org/10.1007/s10980-025-02261-3.
2. Den Hartog, C. Structure, function, and classification in seagrass communities. In *A Scientific Perspective*; McRoy, C.P., Helfferich, C., Eds.; Marcel Dekker: New York, 1977; pp. 89–121.
3. Boudouresque, C.F.; Meinesz, A. Découverte de l'herbier de Posidonies. *Cahier Parc Nation Port-Cros* 1982, *4*, 79 (in French).
4. Edgar, G.J.; Shaw, C. The production and trophic ecology of shallow-water fish assemblages in southern Australia. 3. General relationships between sediments, seagrasses, invertebrates, and fishes. *J. Exp. Mar. Biol. Ecol.* 1995, *194*, 107–131. https://doi.org/10.1016/0022-0981(95)00085-2.
5. Peirano, A.; Damasso, V.; Montefalcone, M.; Morri, C.; Bianchi, C.N. Effects of climate, invasive species, and anthropogenic impacts on the growth of the seagrass *Posidonia oceanica* (L.) Delile in Liguria (NW Mediterranean Sea). *Mar. Pollut. Bull.* 2005, *50*, 817–822. https://doi.org/10.1016/j.marpolbul.2005.02.011.
6. Pergent-Martini, C.; Leoni, V.; Pasqualini, V.; Ardizzone, G.D.; Balestri, E.; Bedini, R.; Belluscio, A.; Belsher, T.; Borg, J.; Boudouresque, C.F.; Boumaza, S.; Bouquegneau, J.M.; Buia, M.C.; Calvo, S.; Cebrian, J.; Charbonnel, E.; Cinelli, F.; Cossu, A.; Maida, G.D.; Dural, B.; Francour, P.; Gobert, S.; Lepoint, G.; Meinesz, A.; Molenaar, H.; Mansour, H.M.; Panayotidis, P.; Peirano, A.; Pergent, G.; Piazzi, L.; Pirrotta, M.; Relini, G.; Romero, J.; Sanchez-Lizaso, J.L.; Semroud, R.; Shembri, P.; Shili, A.; Tomasello, A.; Velimirov, B. Descriptors of *Posidonia oceanica* meadows: Use and application. *Ecol. Indic.* 2005, *5*, 213–230. https://doi.org/10.1016/j.ecolind.2005.02.004.
7. UNEP-MAP-RAC/SPA. Rapport sur l'état de mise en œuvre du Protocole ASP/DB. Document de travail pour la neuvièmeréunion des Points focaux pour les ASP, Floriana, Malte, 3–6 juin 2009, UNEP(DEPI)/MED WG.331/03, CAR/ASP édit., Tunis, 2009; 19p.
8. Boudouresque, C.F.; Bianchi, C.N. Une idée neuve: la protection des espèces marines. In *GIS Posidonie: plus de 30 ans au service de la protection et de la gestion du milieu marin*; Le Direach, L.; Boudouresque, C.F., Eds.; GIS Posidonie: Marseille, 2013; pp. 85–91.
9. Comte, A.; Barreyre, J.; Monnier, B.; de Rafael, R.; Boudouresque, C.-F.; Pergent, G.; Ruitton, S. Operationalizing blue carbon principles in France: Methodological developments for *Posidonia oceanica* seagrass meadows and institutionalization. *Mar. Pollut. Bull.* 2024, *198*, 115822. https://doi.org/10.1016/j.marpolbul.2023.115822.
10. Gobert, S.; Velimirov, B.; Pergent, G.; Pergent-Martini, C.; Walker, D.I. Biology of *Posidonia*. In *Seagrasses: Biology, Ecology and Conservation*; Larkum, A.W.D.; Orth, R.J.; Duarte, C.M., Eds.; Springer: The Netherlands, 2006; pp. 387–408.

 doi:10.20944/preprints202603.1020.v1

11. UNEP/MAP-RAC/SPA. Guidelines for Standardization of Mapping and Monitoring Methods of Marine Magnoliophyta in the Mediterranean; Pergent-Martini, C., Ed.; RAC/SPA: Tunis, 2015; 48p. + Annexes.
12. Mutlu, E.; Olguner, C.; Gökoğlu, M.; Özvarol, Y. Seasonal growth dynamics of *Posidonia oceanica* in a pristine Mediterranean gulf. *Ocean Sci. J.* 2022, *57*, 381–397. https://doi.org/10.1007/s12601-022-00078-8.
13. Mutlu, E.; Karaca, D.; Duman, G.S.; Şahin, A.; Özvarol, Y.; Olguner, C. Seasonality and phenology of an epiphytic calcareous red alga, *Hydrolithon boreale*, on the leaves of *Posidonia oceanica* (L) Delile in the Turkish waters. *Environ. Sci. Pollut. Res.* 2023, *30*, 17193–17213. https://doi.org/10.1007/s11356-022-23333-w.
14. Mutlu, E.; Duman, G.S.; Karaca, D.; Özvarol, Y.; Şahin, A. Biometrical variation of *Posidonia oceanica* with different bottom types along the entire Turkish Mediterranean coast. *Ocean Sci. J.* 2023, *58*, 9. https://doi.org/10.1007/s12601-023-00104-3.
15. Colantoni, P.; Gallignani, P.; Fresi, E.; Cinelli, F. Patterns of *Posidonia oceanica* (L.) Delile beds around the Island of Ischia (Gulf of Naples) and in adjacent waters. *PSZNI: Mar. Ecol.* 1982, *3*, 53–74. https://doi.org/10.1111/j.1439-0485.1982.tb00105.x.
16. Vacchi, M.; Montefalcone, M.; Bianchi, C.N.; Morri, C.; Ferrari, M. Hydrodynamic constraints to the seaward development of *Posidonia oceanica* meadows. *Estuar. Coast. Shelf Sci.* 2012, *97*, 58–65. https://doi.org/10.1016/j.ecss.2011.11.024.
17. Tomasello, A.; Perrone, R.; Colombo, P.; Pirrotta, M.; Calvo, S. Root hair anatomy and morphology in *Posidonia oceanica* (L.) Delile and substratum typology: First observations of a spiral form. *Aquat. Bot.* 2018, *145*, 45–48. https://doi.org/10.1016/j.aquabot.2017.12.001.
18. Catucci, E.; Scardi, M. Modeling *Posidonia oceanica* shoot density and rhizome primary production. *Sci. Rep.* 2020, *10*, 16978. https://doi.org/10.1038/s41598-020-73722-9.
19. Sghaier, Y.R.; Zakhama-Sraieb, R.Y.M.; Charfi-Cheikhrouha, F. Patterns of shallow seagrass (*Posidonia oceanica*) growth and flowering along the Tunisian coast. *Aquat. Bot.* 2013, *104*, 185–192. https://doi.org/10.1016/j.aquabot.2011.09.006.
20. Bonacorsi, M.; Pergent-Martini, C.; Breand, N.; Pergent, G. Is *Posidonia oceanica* regression a general feature in the Mediterranean Sea? *Medit. Mar. Sci.* 2013, *14*, 193–203. https://doi.org/10.12681/mms.334.
21. Alagna, A.; D'Anna, G.; Musco, L.; Fernandez, T.V.; Gresta, M.; Pierozzi, N.; Badalamenti, F. Taking advantage of seagrass recovery potential to develop novel and effective meadow rehabilitation methods. *Mar. Pollut. Bull.* 2019, *149*, 110578. https://doi.org/10.1016/j.marpolbul.2019.110578.
22. Pergent-Martini, C.; Acunto, S.; Andre, S.; Barralon, E.; Calvo, S.; Castejon-Silvo, I.; Culioli, J.M.; Lehman, L.; Molenaar, H.; Monnier, B.; Oberti, P.; Pey, A.; Piazzi, L.; Santoni, M.C.; Terrados, J.; Tomasello, A.; Pergent, G. *Posidonia oceanica* Restoration, a Relevant Strategy after Boat Anchoring Degradation? In *Proceedings of the 7th Mediterranean Symposium on Marine Vegetation*, Genoa, Italy, 19–20 September 2022; RAC/SPA: Tunis, 2022; pp. 78–83.
23. Vacchi, M.; De Falco, G.; Simeone, S.; Montefalcone, M.; Morri, C.; Ferrari, M.; Bianchi, C.N. Biogeomorphology of the Mediterranean *Posidonia oceanica* seagrass meadows. *Earth Surf. Proc. Land.* 2017, *42*, 42–54. https://doi.org/10.1002/esp.3932.
24. Topouzelis, K.; Makri, D.; Stoupas, N.; Papakonstantinou, A.; Katsanevakis, S. Seagrass mapping in Greek territorial waters using Landsat-8 satellite images. *Int. J. Appl. Earth Obs. Geoinf.* 2018, *67*, 98–111.

 doi:10.20944/preprints202603.1020.v1

25. Gerakaris, V.; Papathanasiou, V.; Salomidi, M.; Issaris, Y.; Panayotidis, P. Spatial patterns of *Posidonia oceanica* structural and functional features in the Eastern Mediterranean (Aegean and E. Ionian Seas) in relation to large-scale environmental factors. *Mar. Environ. Res.* 2021, *165*, 105222.
26. Panayotidis, P.; Papathanasiou, V.; Gerakaris, V.; Fakiris, E.; Orfanidis, S.; Papatheodorou, G.; Kosmidou, M.; Georgiou, N.; Drakopoulou, V.; Loukaidi, V. Seagrass meadows in the Greek Seas: presence, abundance and spatial distribution. *Botanica Marina* 2022, *65*, 289–299. https://doi.org/10.1515/bot-2022-0011.
27. Litsi-Mizan, V.; Efthymiadis, P.T.; Gerakaris, V.; Serrano, O.; Tsapakis, M.; Apostolaki, E.T. Decline of seagrass (*Posidonia oceanica*) production over two decades in the face of warming of the Eastern Mediterranean Sea. *New Phytol.* 2023, *239*, 2126–2137. https://doi.org/10.1111/nph.19084.
28. Litsi-Mizan, V.; García-Escudero, C.A.; Tsigenopoulos, C.S.; Tsiaras, K.; Gerakaris, V.; Apostolaki, E.T. Unravelling the genetic pattern of seagrass (*Posidonia oceanica*) meadows in the Eastern Mediterranean Sea. *Biodivers. Conserv.* 2024, *33*, 257–280. https://doi.org/10.1007/s10531-023-02746-0.
29. Pergent, G.; Pergent-Martini, C.; Boudouresque, C.F. Utilisation de l'herbier à *Posidonia oceanica* comme indicateur biologique de la qualité du milieu littoral en Méditerranée: État des connaissances. *Mesogee* 1995, *54*, 3–27.
30. Gobert, S.; Lefebvre, L.; Boissery, P.; Richir, J. A non-destructive method to assess the status of *Posidonia oceanica* meadows. *Ecol. Indic.* 2020, *119*, 106838.
31. Prado, P.; Alcoverro, T.; Romero, J. Influence of nutrients in the feeding ecology of seagrass (*Posidonia oceanica L.*) consumers: a stable isotopes approach. *Mar. Biol.* 2010, *157*, 715–724. https://doi.org/10.1007/s00227-009-1355-2.
32. van Rein, H.; Brown, C.J.; Quinn, R.; Breen, J.; Schoeman, D. An evaluation of acoustic seabed classification techniques for marine biotope monitoring over broad-scales (>1 km²) and meso-scales (10 m²–1 km²). *Estuar. Coast. Shelf Sci.* 2011, *93*, 336–349. https://doi.org/10.1016/j.ecss.2011.04.011.
33. Fakiris, E.; Zoura, D.; Ramfos, A.; Spinos, E.; Georgiou, N.; Ferentinos, G.; Papatheodorou, G. Object-based classification of sub-bottom profiling data for benthic habitat mapping. Comparison with sidescan and RoxAnn in a Greek shallow-water habitat. *Estuar. Coast. Shelf Sci.* 2018, *208*, 219–234. https://doi.org/10.1016/j.ecss.2018.04.028.
34. Lee, W.S.; Lin, C.Y. Mapping of tropical marine benthic habitat: Hydroacoustic classification of coral reefs environment using single-beam (RoxAnn™) system. *Cont. Shelf Res.* 2018, *170*, 1–10.
35. Dimas, X.; Fakiris, E.; Christodoulou, D.; Georgiou, N.; Geraga, M.; Papathanasiou, V.; Orfanidis, S.; Kotomatas, S.; Papatheodorou, G. Marine priority habitat mapping in a Mediterranean conservation area (Gyaros, South Aegean) through multi-platform marine remote sensing techniques. *Front. Mar. Sci.* 2022, *9*, 953462. https://doi.org/10.3389/fmars.2022.953462.
36. Dattola, L.; Rende, S.F.; Dominici, R.; Lanera, P.; Di Men, R.; Scalise, S.; Cappa, P.; Oranges, T.; Aramini, G. Comparison of Sentinel-2 and Landsat-8 OLI satellite images vs. high spatial resolution images (MIVIS and WorldView-2) for mapping *Posidonia oceanica* meadows. In *Proceedings of SPIE 10784, Remote Sensing of the Ocean, Sea Ice, Coastal Waters, and Large Water Regions*, 1078419, 2018. https://doi.org/10.1117/12.2326798.
37. Yücel-Gier, G.; Koçak, G.; Akçalı, B.; İlhan, T.; Duman, M. Evaluation of *Posidonia oceanica* Map Generated by Sentinel-2 Image: Gülbahçe Bay Test Site. *TrJFAS* 2020, *20*, 571–581. https://doi.org/10.4194/1303-2712-v20_7_07.

 doi:10.20944/preprints202603.1020.v1

38. Traganos, D.; Aggarwal, B.; Poursanidis, D.; Topouzelis, K.; Chrysoulakis, N.; Reinartz, P. Towards global-scale seagrass mapping and monitoring using Sentinel-2 on Google Earth Engine: The case study of the Aegean and Ionian Seas. *Remote Sens.* 2018, *10*, 1227. https://doi.org/10.3390/rs10081227.
39. Mederos-Barrera, A.; Marcello, J.; Eugenio, F.; Hernández, E. Seagrass mapping using high resolution multispectral satellite imagery: A comparison of water column correction models. *Int. J. Appl. Earth Obs. Geoinf.* 2022, *113*, 102990. https://doi.org/10.1016/j.jag.2022.102990.
40. McCarthy, E.; Sabol, B. Acoustic characterization of submerged aquatic vegetation: military and environmental monitoring applications. In *Oceans 2000 MTS/IEEE Conference and Exhibition*, Providence, USA, 2000; pp. 1957–1961.
41. Vis, C.; Hudon, C.; Carignan, R. An evaluation of approaches used to determine the distribution and biomass of emergent and submerged aquatic macrophytes over large spatial scales. *Aquat. Bot.* 2003, *77*, 187–201.
42. Brown, C.J.; Smith, S.J.; Lawton, P.; Anderson, J.T. Benthic habitat mapping: A review of progress towards improved understanding of the spatial ecology of the seafloor using acoustic techniques. *Estuar. Coast. Shelf Sci.* 2011, *92*, 502–520.
43. Hossain, M.S.; Mazlan, H. Potential of Earth Observation (EO) technologies for seagrass ecosystem service assessments. *Int. J. Appl. Earth Obs. Geoinf.* 2019, *77*, 15–29. https://doi.org/10.1016/j.jag.2018.12.009.
44. Pasqualini, V.; Pergent-Martini, C.; Clabaut, P.; Pergent, G. Mapping of *Posidonia oceanica* using aerial photographs and side-scan sonar: application to the island of Corsica (France). *Estuar. Coast. Shelf Sci.* 1998, *47*, 359–367.
45. Di Maida, G.; Tomasello, A.; Luzzu, F.; Scannavino, A.; Pirrotta, M.; Orestano, C.; Calvo, S. Discriminating between *Posidonia oceanica* meadows and sand substratum using multibeam sonar. *ICES J. Mar. Sci.* 2011, *68*, 12–19. https://doi.org/10.1093/icesjms/fsq130.
46. Mutlu, E. Acoustical identification of the concentration layer of a copepod species, *Calanus euxinus*. *Mar. Biol.* 2003, *142*, 517–523. https://doi.org/10.1007/s00227-002-0986-3.
47. Mutlu, E. Diel vertical migration of *Sagitta setosa* as inferred acoustically in the Black Sea. *Mar. Biol.* 2006, *149*, 573–584. https://doi.org/10.1007/s00227-005-0221-0.
48. Lavery, A.C.; Wiebe, P.H.; Stanton, T.K.; Lawson, G.L.; Benfield, M.C.; Copley, N. Determining dominant scatterers of sound in mixed zooplankton populations. *J. Acoust. Soc. Am.* 2007, *122*, 3304–3326.
49. Mutlu, E. A package of script codes, POSIBIOM, for vegetation acoustics: POSIdonia BIOMass. *J. Mar. Sci. Eng.* 2023, *11*, 1790. https://doi.org/10.3390/jmse11091790.
50. Mutlu, E.; Olguner, C. Acoustic scattering properties of seagrass: In/ex situ measurements of *Posidonia oceanica*. *Medit. Mar. Sci.* 2023, *24*, 272–291. https://doi.org/10.12681/mms.32324.
51. Mutlu, E.; Olguner, C. Acoustic scattering properties of a seagrass, *Cymodocea nodosa*: In-situ measurements. *Bot. Mar.* 2023, *6*, 491–505. https://doi.org/10.1515/bot-2022-0083.
52. Carbó, R.; Molero, A.C. Scattering strength of a *Gelidium* biomass bottom. *Appl. Acoust.* 1997, *51*, 343–351. https://doi.org/10.1016/S0003-682X(97)00012-1.
53. Shao, H.; Minami, K.; Shirakawa, H.; Kawauchi, Y.; Matsukura, R.; Tomiyasu, M.; Miyashita, K. Target strength of a common kelp species, *Saccharina japonica*, measured using a quantitative echosounder in an indoor seawater tank. *Fish. Res.* 2019, *214*, 110–116. https://doi.org/10.1016/j.fishres.2019.01.009.

 doi:10.20944/preprints202603.1020.v1

54. Llorens-Escrich, S.; Tamarit, E.; Hernandis, S.; Sánchez-Carnero, N.; Rodilla, M.; Pérez-Arjona, I.; Moszynski, M.; Puig-Pons, V.; Tena-Medialdea, J.; Espinosa, V. Vertical configuration of a side scan sonar for the monitoring of *Posidonia oceanica* meadows. *J. Mar. Sci. Eng.* 2021, *9*, 1332. https://doi.org/10.3390/jmse9121332.
55. Minami, K.; Kita, C.; Shirakawa, H.; Kawauchi, Y.; Shao, H.; Tomiyasu, M.; Iwahara, Y.; Takahara, H.; Kitagawa, T.; Miyashita, K. Acoustic characteristics of a potentially important macroalgae, *Sargassum horneri*, for coastal fisheries. *Fish. Res.* 2021, *240*, 105955. https://doi.org/10.1016/j.fishres.2021.105955.
56. Mutlu, E.; Balaban, C. New algorithms for the acoustic biomass estimation of *Posidonia oceanica*: A study in the Antalya Gulf (Turkey). *Fresenius Environ. Bull.* 2018, *27*, 2555–2561.
57. Mutlu, E.; Olguner, C. Density-dependent acoustical identification of two common seaweeds (*Posidonia oceanica* and *Cymodocea nodosa*) in the Mediterranean Sea. *Thalassas* 2023, *39*, 1155–1167. https://doi.org/10.1007/s41208-023-00533-w.
58. Mutlu, E.; Olguner, C.; Özvarol, Y.; Gökoğlu, M. A preliminary study on acoustic-based estimation of biometric parameters of *Posidonia oceanica*. *Thalassas* 2026, (under 2nd review).
59. Mutlu, E.; Özvarol, Y.; Akçalı, B.; Aslan, B.E.; Seçkiner, S. Determination of distributional maximum biomass (summer) of *Posidonia oceanica* along the Turkish waters of the Aegean Sea and its seasonal dynamics in Side's bed (Antalya, Mediterranean Sea) using the acoustic method. *TÜBİTAK Project*, grant no: 124Y031, 2nd Interim report, Ankara, Turkey, pp. 64 (in progress).
60. Mutlu, E.; Olguner, C.; Özvarol, Y.; Gökoğlu, M. Spatiotemporal biometrics of *Cymodocea nodosa* in a western Turkish Mediterranean coast. *Biologia* 2022, *77*, 649–670. https://doi.org/10.1007/s11756-021-00953-0.
61. Mutlu, E.; Özvarol, Y.; Akçalı, B.; Aslan, B.E.; Seçkiner, S. Determination of distributional maximum biomass (summer) of *Posidonia oceanica* along the Turkish waters of the Aegean Sea and its seasonal dynamics in Side's bed (Antalya, Mediterranean Sea) using the acoustic method. *TÜBİTAK Project*, grant no: 124Y031, 1st Interim Report, Ankara, Turkey, pp. 127 (in progress).
62. Mutlu, E.; Olguner, C.; Gökoğlu, M.; Özvarol, Y. Population dynamics and ecology of *Caulerpa prolifera* vs *Caulerpa taxifolia* var. distichophylla within a Levantine Gulf. *Thalassas* 2022, *38*, 1311–1325. https://doi.org/10.1007/s41208-022-00477-7.
63. Mavko, G.; Mukerji, T.; Dvorkin, J. *The Rock Physics Handbook*, 2nd ed.; Cambridge University Press: Cambridge, UK, 1998.
64. Aleman, P.B. Acoustic impedance inversion of lower Permian carbonate buildups in the Permian Basin, Texas. Master's Thesis, Texas A&M University, 2004; 99.
65. Enriquez, S.; Schubert, N. Direct contribution of the seagrass *Thalassia testudinum* to lime mud production. *Nat. Commun.* 2004, *I*, 3835. https://doi.org/10.1038/ncomms4835.
66. Balestri, E.; Cinelli, F. Sexual reproductive success in *Posidonia oceanica*. *Aquatic Bot.* 2003, *75*, 21–32. https://doi.org/10.1016/S0304-3770(02)00151-1.
67. Balestri, E.; de Battisti, D.; Vallerini, F.; Lardicci, C. First evidence of root morphological and architectural variations in young *Posidonia oceanica* plants colonizing different substrate typologies. *Estuar. Coast. Shelf Sci.* 2015, *154*, 205–213. https://doi.org/10.1016/j.ecss.2015.01.002.
68. Pereda-Briones, L.; Infantes, E.; Orfila, A.; Tomas, F.; Terrados, J. Dispersal of seagrass propagules: Interaction between hydrodynamics and substratum type. *Mar. Ecol. Prog. Ser.* 2018, *593*, 47–59. https://doi.org/10.3354/meps12518.

 doi:10.20944/preprints202603.1020.v1

69. Marba, N.; Duarte, C.M.; Holmer, M.; Martínez, R.; Basterretxea, G.; Orfila, A.; Jordi, A.; Tintoré, J. Effectiveness of protection of seagrass (*Posidonia oceanica*) populations in Cabrera National Park (Spain). *Environ. Conserv.* 2002, *29*, 509–518. https://doi.org/10.1017/S037689290200036X.
70. De Falco, G.; Baroli, M.; Cucco, A.; Simeone, S. Intrabasinal conditions promoting the development of a biogenic carbonate sedimentary facies associated with the seagrass *Posidonia oceanica*. *Cont. Shelf Res.* 2008, *28*, 797–812. https://doi.org/10.1016/j.csr.2007.12.014.
71. Montefalcone, M.; Vacchi, M.; Archetti, R.; Ardizzone, G.; Astruch, P.; Bianchi, C.N.; Calvo, S.; Criscoli, A.; Fernandez-Torquemada, Y.; Luzzu, F.; Misson, G.; Morri, C.; Pergent, G.; Tomasello, A.; Ferrari, M. Geospatial modelling and map analysis allowed measuring regression of the upper limit of *Posidonia oceanica* seagrass meadows under human pressure. *Estuar. Coast. Shelf Sci.* 2019, *217*, 148–157. https://doi.org/10.1016/j.ecss.2018.11.006.
72. Yalçın, M.G.; Mutlu, E.; Olguner, C.; Atakoğlu, ÖÖ.; Bat, L.; Özkan, E.Y. Spatial geochemical structure of soft sediment on shallow littoral of the Gulf of Antalya, the eastern Mediterranean Sea. *Mar. Poll. Bull.* 2023, *193*, 115155. https://doi.org/10.1016/j.marpolbul.2023.115155.
73. Milliman, J.D. Production and accumulation of calcium carbonate in the ocean: Budget of a nonsteady state. *Glob. Biogeochem. Cyc.* 1993, *7*, 927–957. https://doi.org/10.1029/93GB02524.
74. Canals, M.; Ballesteros, E. Production of carbonate particles by phytobenthic communities on the Mallorca-Menorca shelf, northwestern Mediterranean Sea. *Deep-Sea Res. II* 1997, *44*, 611–629.
75. Gnisci, V.; Martiis, S.C.; Belmonte, A.; Micheli, C.; Piermattei, V.; Bonamano, S.; Marcelli, M. Assessment of the ecological structure of *Posidonia oceanica* (L.) Delile on the northern coast of Lazio, Italy (central Tyrrhenian, Mediterranean). *Ital. Bot.* 2020, *9*, 1–19. https://doi.org/10.3897/italianbotanist.9.46426.
76. Sandoval-Gil, J.M.; Ruiz, J.M.; Marín-Guirao, L.; Bernardeau-Esteller, J.; Sánchez-Lizaso, J.L. Ecophysiological plasticity of shallow and deep populations of the Mediterranean seagrasses *Posidonia oceanica* and *Cymodocea nodosa* in response to hypersaline stress. *Mar. Environ. Res.* 2014, *95*, 39–61. https://doi.org/10.1016/j.marenvres.2013.12.011.
77. Lal, A.; Arthur, R.; Marba, N.; Lill, A.W.T.; Alcoverro, T. Implications of conserving an ecosystem modifier: increasing green turtle (*Chelonia mydas*) densities substantially alters seagrass meadows. *Biol. Conserv.* 2010, *143*, 2730–2738. https://doi.org/10.1016/j.biocon.2010.07.020.
78. Steele, L.; Darnell, K.M.; Cebrian, J.; Sanchez-Lizaso, J.L. *Sarpa salpa* herbivory on shallow reaches of *Posidonia oceanica* beds. *Anim. Biodiv. Conserv.* 2014, *37*, 49–57.
79. Marba, N.; Duarte, C.M.; Cebrian, J.; Gallegos, M.E.; Olesen, B.; Sand-Jensen, K. Growth and population dynamics of *Posidonia oceanica* on the Spanish Mediterranean coast: elucidating seagrass decline. *Mar. Ecol. Prog. Ser.* 1996, *137*, 203–213. https://doi.org/10.3354/meps137203.
80. Guidetti, P.; Lorenti, M.; Buia, M.C.; Mazzella, L. Temporal dynamics and biomass partitioning in three Adriatic seagrass species, *Posidonia oceanica*, *Cymodocea nodosa*, *Zostera marina*. *PSZNI Mar. Ecol.* 2002, *23*, 51–67. https://doi.org/10.1046/j.1439-0485.2002.02722.x.
81. Bay, D. A field study of the growth dynamics and productivity of *Posidonia oceanica* (L.) Delile in Calvi Bay, Corsica. *Aquat. Bot.* 1984, *20*, 43–64. https://doi.org/10.1016/0304-3770(84)90026-3.
82. Wittmann, K.J. Temporal and morphological variations of growth in a natural stand of *Posidonia oceanica* (L.) Delile. *Mar. Ecol.* 1984, *5*, 301–316. https://doi.org/10.1111/j.1439-0485.1984.tb00128.x.

 doi:10.20944/preprints202603.1020.v1

83. Sgorbini, S.; Peirano, A.; Cocito, S.; Morgigni, M. An underwater tracking system for mapping marine communities: An application to *Posidonia oceanica*. *Oceanol. Acta* 2002, *25*, 135–138. https://doi.org/10.1016/S0399-1784(02)01188-X.
84. Gobert, S.; Kyramarios, M.; Lepoint, G.; Pergent-Martini, C.J.; Bouquegneau, J.-M. Variations at different spatial scales of the *Posidonia oceanica* (L.) Delile meadow; effects on the physicochemical parameters of the sediment. *Oceanol. Acta* 2003, *26*, 199–207.
85. Maida, G.D.I.; Tomasello, A.; Sciandra, M.; Pirrotta, M.; Milazzo, M.; Calvo, S. Effect of different substrata on rhizome growth, leaf biometry and shoot density of *Posidonia oceanica*. *Mar. Environ. Res.* 2013, *87–88*, 96–102. https://doi.org/10.1016/j.marenvres.2013.04.001.
86. Giovannetti, E.; Lasagna, R.; Montefalcone, M.; Bianchi, C.N.; Albertelli, G.; Morri, C. Inconsistent responses to substratum nature in *Posidonia oceanica* meadows: An integration through complexity levels? *Chem. Ecol.* 2008, *24*, S83–S91. https://doi.org/10.1080/02757540801966439.
87. Touchette, B.W.; Burkholder, J.M. Overview of the physiological ecology of carbon metabolism in seagrasses. *J. Exp. Mar. Biol. Ecol.* 2000, *250*, 169–205. https://doi.org/10.1016/S0022-0981(00)00196-9.
88. Perez, M.; Duarte, C.M.; Romero, J.; Sand-Jensen, K.; Alcoverro, T. Growth plasticity in *Cymodocea nodosa* stands: The importance of nutrient supply. *Aquat. Bot.* 1994, *47*, 249–264. https://doi.org/10.1016/0304-3770(94)90056-6.
89. Marbà, N.; Duarte, C.M. Rhizome elongation and seagrass clonal growth. *Mar. Ecol.-Prog. Ser.* 1998, *255*, 127–134. https://doi.org/10.3354/MEPS174269.
90. Fernandez-Torquemada, Y.; Sanchez-Lizaso, J.L. Effects of salinity on leaf growth and survival of the Mediterranean seagrass *Posidonia oceanica* (L.) Delile. *J. Exp. Mar. Biol. Ecol.* 2005, *320*, 57–63. https://doi.org/10.1016/j.jembe.2004.12.019.
91. Via, J.D.; Sturmbauer, C.; Schonweger, G.; Sotz, E.; Mathekowitsch, S.; Stifter, M.; Rieger, R. Light gradients and meadow structure in *Posidonia oceanica*: Ecomorphological and functional correlates. *Mar. Ecol.-Prog. Ser.* 1998, *163*, 267–278. https://doi.org/10.3354/meps163267.
92. Sghaier, Y.R.; Zakhama-Sraieb, R.; Charfi-Cheikhrouha, F. Status of *Posidonia oceanica* along eastern coast of Tunisia. *Biol. Mar. Medit.* 2006, *13*, 85–91.
93. Dalmau, A.; Gubbay, S.; Garcia-Herrero, A. *Posidonia beds* (*Posidonion oceanicae*) (1120*). In: Olmeda, C.; Šefferová Stanová, V. (Eds.) Technical guidelines for assessing and monitoring the condition of Annex I habitat types of the Directive 92/43/EEC; Publications Office of the European Union: Luxembourg, 2025; ISBN 978-92-68-32012-9. https://doi.org/10.2779/0249500.
94. Mutlu, E.; Gökoğlu, M.; Özvarol, Y.; Balaban, C.; Olguner, M.T. Yaygın deniz çayırlarının akustiksel yoğunluk kalibrasyonu ve dağılımlarının takip edilmesi [Acoustical density-dependent calibration of the dominant sea meadows and seagrasses and monitoring of their distribution]. Final Report, TUBITAK, no: 110Y232, Ankara, Turkey, 2014, pp. 337.
95. Mutlu, E.; Meo, I.d.; Miglietta, C.; Deval, M.C. Ecological Indicative Stressors of Native vs Non-Native Fish in an Ultra-Oligotrophic Region of the Mediterranean Sea. *Sustainability* 2023, *15*, 2726. https://doi.org/10.3390/su15032726.
96. Stanton, T.K.; Chu, D.; Wiebe, P.H. Acoustic scattering characteristics of several zooplankton groups. *ICES J. Mar. Sci.* 1996, *53*, 289–295.
97. Simmonds, J.; Maclennan, D. *Fisheries acoustics: Theory and practice*, 2nd ed.; Blackwell Publishing: 2005; pp. 456.

 doi:10.20944/preprints202603.1020.v1

98. Alcoverro, T.; Romero, J.C.M.; Duarte, N.; Lopez, L. Spatial and temporal variations in nutrient limitation of seagrass *Posidonia oceanica* growth in the NW Mediterranean. *Mar. Ecol. Prog. Ser.* 1997, *146*, 155–161. https://doi.org/10.3354/meps146155.
99. Pirc, H. Seasonal aspects of photosynthesis in *Posidonia oceanica*: Influence of depth, temperature, and light intensity. *Aquat. Bot.* 1986, *26*, 203–212. https://doi.org/10.1016/0304-3770(86)90021-5.
100. Ruiz, J.M.; Romero, J. Effects of in situ experimental shading on the Mediterranean seagrass *Posidonia oceanica*. *Mar. Ecol.-Prog. Ser.* 2001, *215*, 107–120. https://doi.org/10.3354/meps215107.
101. Mateo, M.A.; Romero, J.; Perez, M.; Littler, M.M.; Littler, D.S. Dynamics of millenary organic deposits resulting from the growth of the Mediterranean seagrass *Posidonia oceanica*. *Estuar. Coast. Shelf Sci.* 1997, *44*, 103–110. https://doi.org/10.1006/ecss.1996.0116.
102. Merriam, C.O. Depositional history of lower Permian (Wolfcampian - Leonardian) carbonate buildups, Midland Basin, Upton County, Texas. M.S. thesis, Texas A&M University, 1999.
103. Karaca, D.; Mutlu, E.; Uysal, Z. Summer surface phytoplankton assemblages along physically discrete water masses of the entire Turkish Mediterranean coast. *Thalassas* 2026, (in press).
104. Lepoint, G.; Defawe, O.; Gobert, S.; Dauby, P.; Bouquegneau, J.-M. Experimental evidence for nitrogen recycling in the leaves of the seagrass *Posidonia oceanica*. *J. Sea Res.* 2002, *48*, 173–179. https://doi.org/10.1016/S1385-1101(02)00164-8.
105. Marín-Guirao, L.; Sandoval-Gil, J.M.; Bernardeau-Esteller, J.; Ruiz, J.M.; Sánchez-Lizaso, J.L. Responses of the Mediterranean seagrass *Posidonia oceanica* to hypersaline stress duration and recovery. *Mar. Environ. Res.* 2013, *84*, 60–75. https://doi.org/10.1016/j.marenvres.2012.12.001.

 doi:10.20944/preprints202603.1020.v1

107. Appendix

108.

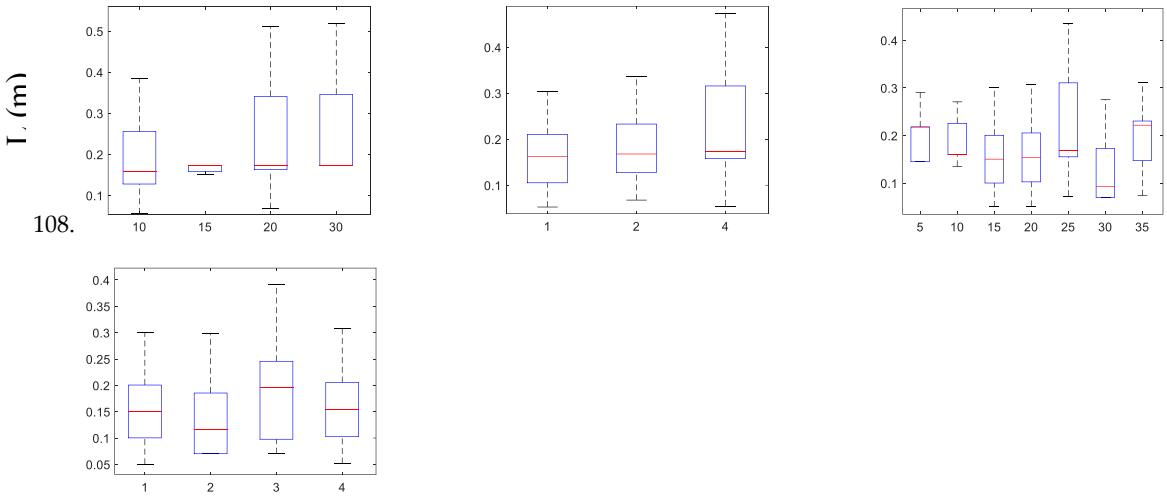

109.

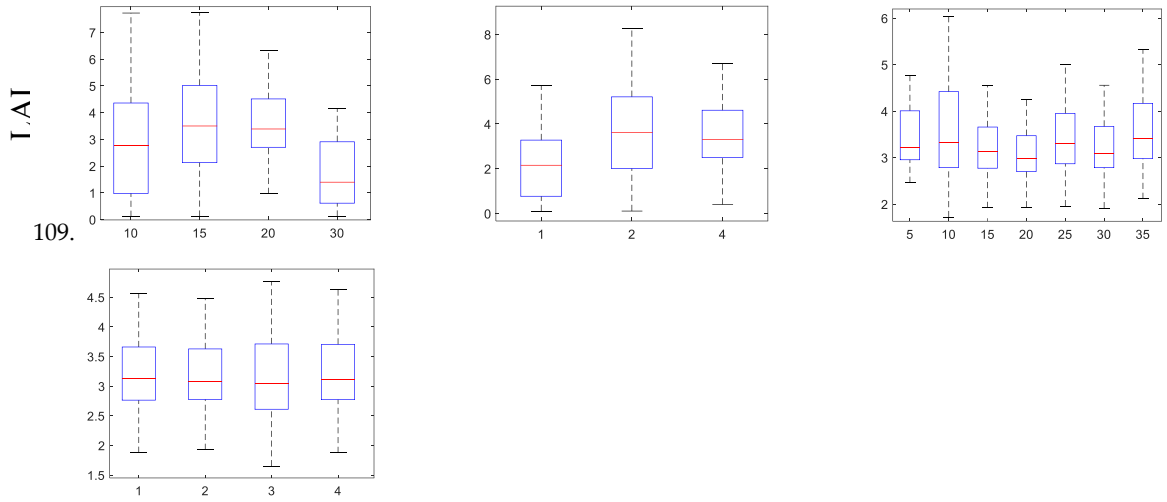

110.

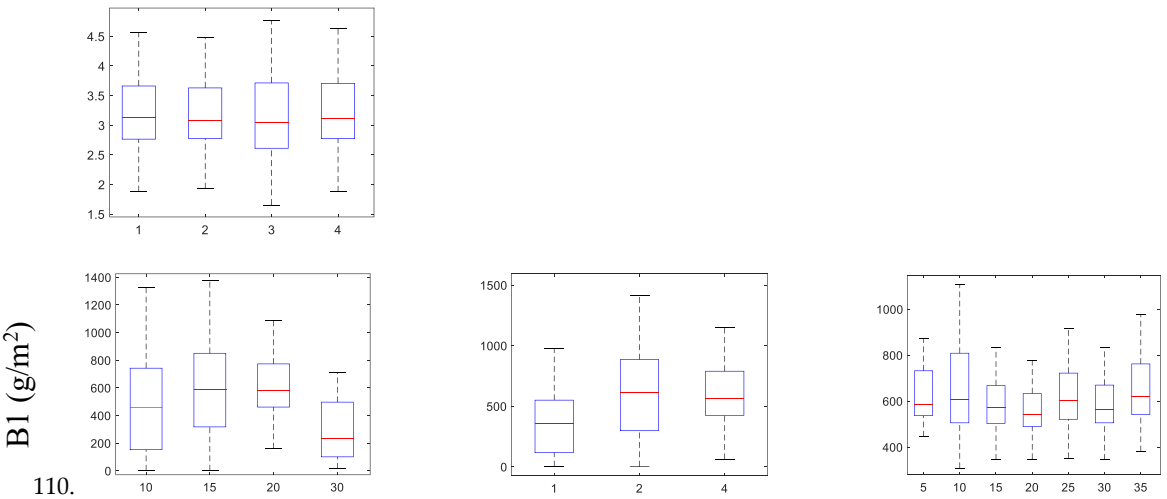

 doi:10.20944/preprints202603.1020.v1

111.

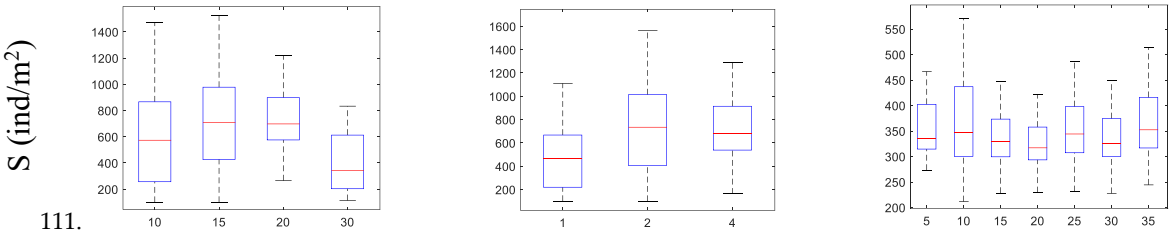

112.

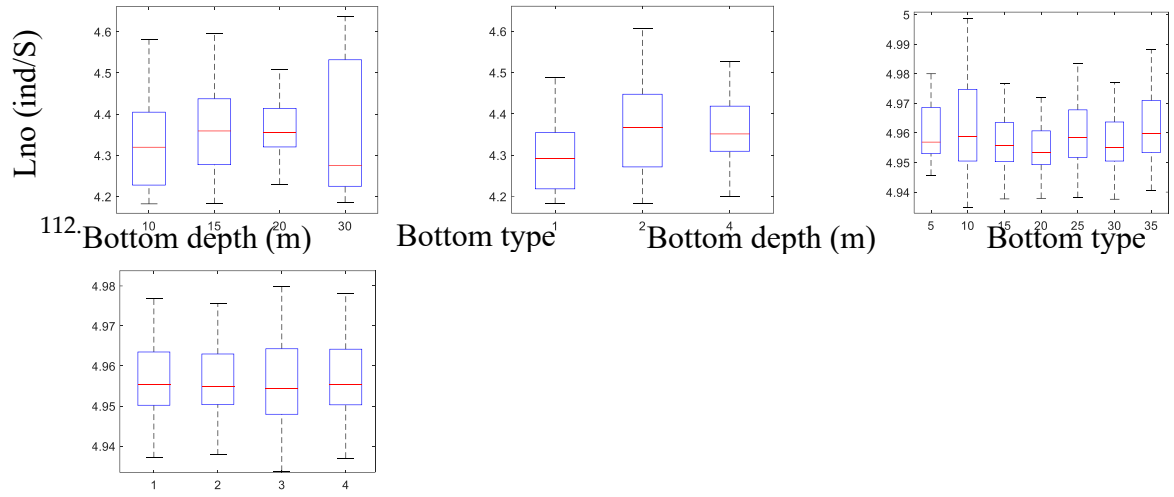

113. **FigureA1.** Regarding only SCUBA sampling stations, box plot of the biometrics estimated from acoustic sampling by bottom depths and bottom types (1: rock, 2: sand, 3: *matte* and 4: mud) in winter and summer, respectively.

 doi:10.20944/preprints202603.1020.v1

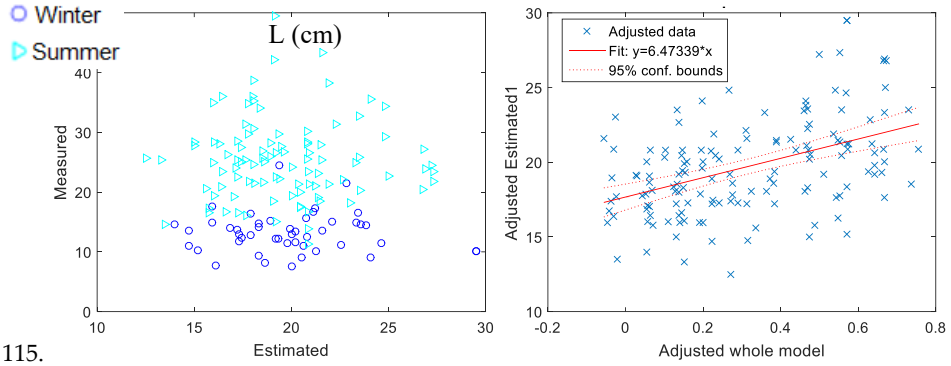

115.

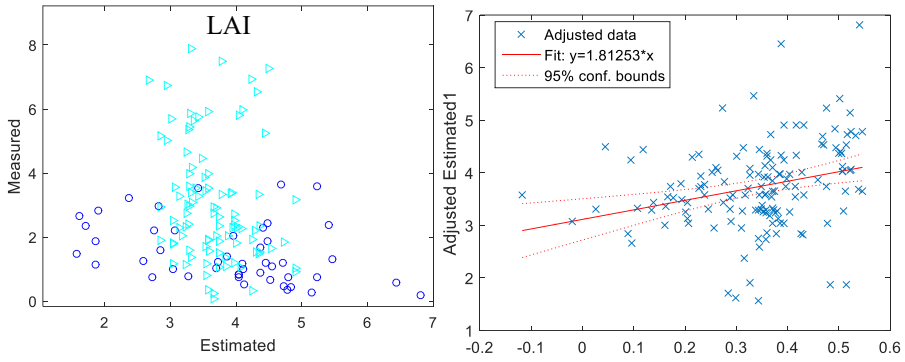

116.

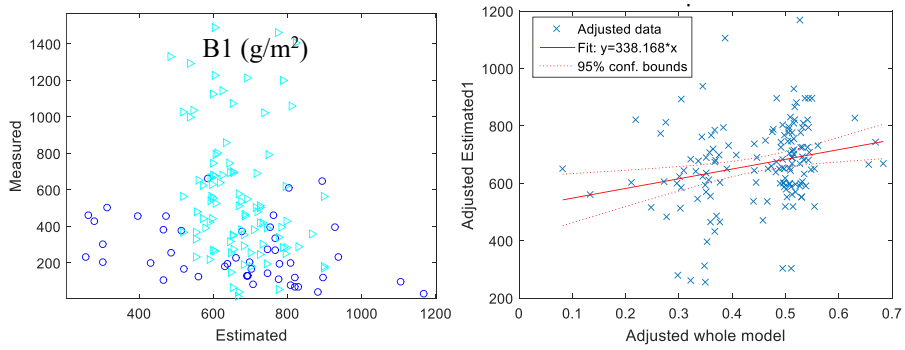

117.

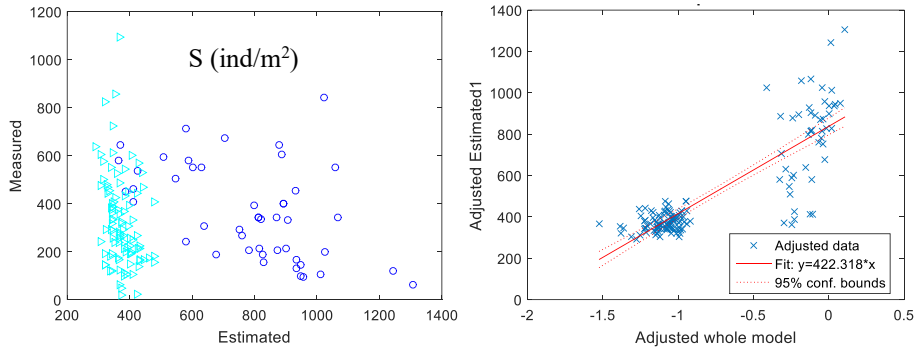

118.

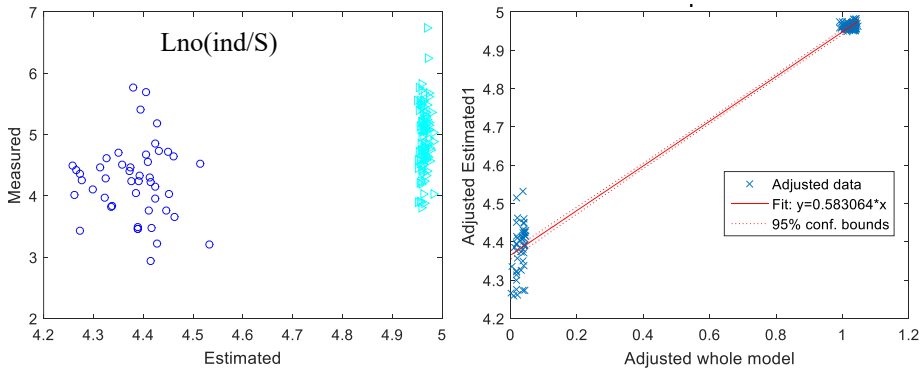

119.

 doi:10.20944/preprints202603.1020.v1

120. **Figure A2.** Plot of the individual measured vs estimated values on a Cartesian axis by months (a) and linear regression model: Estimated ~ 1 + Measured + Month + Depth + Type (b).

121. **Table A1** A Table for reporting a multiple linear regression model with three explanatory variables in fit linear regression model of Estimated ~ 1 + Measured + Month + Depth + Type using formula (Wilkinson's Notation).

122.	123.	124.	125.	126.	127.	128.	129.	130.	131. 132.
133.	134.	135.	136.	137.	138.	139.	140.	141.	142. 143.
144. (Intercept)	145.	146.	147.	148.	149.	150.	151.	152.	153. 154.
155. Measured	156.	157.	158.	159.	160.	161.	162.	163.	164. 165.
166. Season	167.	168.	169.	170.	171.	172.	173.	174.	175. 176.

 doi:10.20944/preprints202603.1020.v1

_Sdepth_10 177. 178. 179. 180. 181. 182. 183. 184. 185. 186. 187.
depth_15 188. 189. 190. 191. 192. 193. 194. 195. 196. 197. 198.
depth_20 199. 200. 201. 202. 203. 204. 205. 206. 207. 208. 209.
depth_25 210. 211. 212. 213. 214. 215. 216. 217. 218. 219. 220.
depth_30 221. 222. 223. 224. 225. 226. 227. 228. 229. 230. 231.

 doi:10.20944/preprints202603.1020.v1

232. Depth_35	233.	234.	235.	236.	237.	238.	239.	240.	241.	242.
243. Type_2	244.	245.	246.	247.	248.	249.	250.	251.	252.	253.
254. Type_3	255.	256.	257.	258.	259.	260.	261.	262.	263.	264.
265. Type_4	266.	267.	268.	269.	270.	271.	272.	273.	274.	275.
276. R^2	277.	278.	279.	280.	281.	282.	283.	284.	285.	286.
287. Adjusted R^2	288.	289.	290.	291.	292.	293.	294.	295.	296.	297.

 doi:10.20944/preprints202603.1020.v1

								307.	
						305.			
	299.		301.		303.				
298. p									
M		300.		302.		304.		306.	308.

309. **Table A2** A Table for reporting a multiple linear regression model with three explanatory variables in robust fitting model of Estimated ~ 1 + Measured + Season + Type + Depth.

			313.					319.	
					315.				
310.	311.	312.		314.		316.	317.	318.	320.
	322.		324.		326.		328.	330.	
		323.		325.		327.		329.	331.
321.									
332. (Intercept)									342.
		334.		336.		338.		340.	
	333.		335.		337.		339.	341.	
343. Measured									
		345.	346.	347.		349.		351.	352. 353.
	344.				348.		350.		

 doi:10.20944/preprints202603.1020.v1

354. Seasonal 355. 356. 357. 358. 359. 360. 361. 362. 363. 364.

365. Type 366. 367. 368. 369. 370. 371. 372. 373. 374. 375.

376. Depth 377. 378. 379. 380. 381. 382. 383. 384. 385. 386.

387. R^2 388. 389. 390. 391. 392. 393. 394. 395. 396. 397.

398. Adjusted R^2 399. 400. 401. 402. 403. 404. 405. 406. 407. 408.

409. pM 410. 411. 412. 413. 414. 415. 416. 417. 418. 419.

 doi:10.20944/preprints202603.1020.v1